Draft of January 11, 2012
Preprint typeset using LaTeX style emulateapj v. 5/2/11

ASTEROID ROTATION PERIODS FROM THE PALOMAR TRANSIENT FACTORY SURVEY

D. Polishook[1], E. O. Ofek[1], A. Waszczak[2], S.R. Kulkarni[2], A. Gal-Yam[1], O. Aharonson[1], R. Laher[3], J. Surace[3], C. Klein[4], J. Bloom[4], N. Brosch[5], D. Prialnik[5], C. Grillmair[6], S.B. Cenko[4], M. Kasliwal[2], N. Law[7], D. Levitan[2], P. Nugent[8], D. Poznanski[4,5,8,9], R. Quimby[2]

Draft of January 11, 2012

ABSTRACT

The Palomar Transient Factory (PTF) is a synoptic survey designed to explore the transient and variable sky in a wide variety of cadences. We use PTF observations of fields that were observed multiple times ($\gtrsim 10$) per night, for several nights, to find asteroids, construct their lightcurves and measure their rotation periods. Here we describe the pipeline we use to achieve these goals and present the results from the first four (overlapping) PTF fields analyzed as part of this program. These fields, which cover an area of 21 deg^2, were observed on four nights with a cadence of ~ 20 min. Our pipeline was able to detect 624 asteroids, of which 145 ($\approx 20\%$) were previously unknown. We present high quality rotation periods for 88 main-belt asteroids and possible period or lower limit on the period for an additional 85 asteroids. For the remaining 451 asteroids, we present lower limits on their photometric amplitudes. Three of the asteroids have lightcurves that are characteristic of binary asteroids. We estimate that implementing our search for all existing high-cadence PTF data will provide rotation periods for about 10,000 asteroids mainly in the magnitude range ≈ 14 to ≈ 20.

Subject headings: minor planets, asteroids: general, surveys: PTF

1. INTRODUCTION

We can use time-series photometry of asteroids and other types of minor planets to study a wide variety of their physical characteristics. The rotation period (spin) can be derived from periodicity in their lightcurves (e.g., Harris et al. 1989); the lightcurve structure and changes in their mean amplitude as a function of viewing angle allow us to reconstruct their shapes (e.g., Kaasalainen & Torppa 2001); and it provides a method to search for binary asteroids (e.g., Polishook et al. 2011). In some cases, the presence of satellites allows the determination of the mass and/or density of the asteroids (e.g., Gnat & Sari 2010). Furthermore, and most relevant to our work, statistics of asteroid rotation periods can be used to understand the physical mechanisms that shape their rotation periods – presumably, the two main mechanisms involved are collisions (Davis et al. 2002) and the thermal Yarkovsky-O'Keefe-Radzievskii-Paddack (YORP) effect (Rubincam 2000).

To date, there are $\approx 3,700$ asteroids with published lightcurves and rotation periods (Warner et al. 2009). Rotation periods of asteroids are typically derived from multiple photometric observations of the same object taken on several nights. Significant contributions were made by amateur astronomers with modest equipment. In recent years, wide-field CCDs provide photometric measurements of many asteroids simultaneously, by dedicated surveys (e.g., Masiero et al. 2009; Polishook and Brosch 2009), or as part of multipurpose surveys, such as the Sloan Digital Sky Survey (SDSS; Ivezić et al. 2001; Ofek 2011). Observations using 1–2 m class telescopes can deliver the rotation periods for ≈ 1 km-size main-belt asteroids. Such small asteroids are particularly interesting since the timescale of physical mechanisms, such as the YORP effect is relatively short, about 10^6 years (Rubincam 2000; Vokrouhlický & Čapek 2002).

Herein we describe a pipeline designed to detect asteroids, construct their lightcurves and measure their rotation periods, in data obtained by the Palomar Transient Factory (PTF[10]; Law et al. 2009; Rau et al. 2009). The PTF is an automated, wide-field survey aimed at a systematic exploration of the optical transient sky. Operating daily, the survey uses a camera with a 7.26 deg^2 field of view assembled on the 1.2-m Oschin telescope at Palomar Observatory (Rahmer et al. 2008). The camera is a mosaic of 11 CCDs, with pixel scale of $1.01'' \mathrm{pix}^{-1}$ (e.g., Figure 1). With an exposure time of 60 s the survey reaches a limiting magnitude of ~ 21 mag with a median seeing of $\approx 2''$. The two filters frequently used are Mould-R and SDSS-g'. The PTF survey samples the sky in a variety of cadences to match the scientific goals of different programs, such as the search for supernovae (e.g., Arcavi et al. 2010) and galactic variables (e.g. Levitan et al. 2011). Part of the PTF time is used for high cadence observations, in which we obtain $\gtrsim 20$ observations of the same field in a given night, and in some cases we repeat these high cadence observations on

[1] Benoziyo Center for Astrophysics, Weizmann Institute of Science, 76100 Rehovot, Israel.
[2] Division of Physics, Mathematics and Astronomy, California Institute of Technology, Pasadena, CA 91125, USA.
[3] Spitzer Science Center, California Institute of Technology, M/S 314-6, Pasadena, CA 91125, U.S.A.
[4] Department of Astronomy, University of California, Berkeley, CA, 94720-3411, USA.
[5] Faculty of Exact Sciences, Tel-Aviv University, 69978 Tel-Aviv-Yafo, Israel.
[6] Infrared Processing and Analysis Center, California Institute of Technology, M/S 100-22, Pasadena, CA 91125, U.S.A.
[7] Dunlap Institute for Astronomy and Astrophysics, University of Toronto, Toronto, M5S 3H4 Ontario, Canada.
[8] Computational Cosmology Center, Lawrence Berkeley National Laboratory, Berkeley, CA 94720, USA.
[9] Einstein Fellow.

[10] http://www.astro.caltech.edu/ptf/

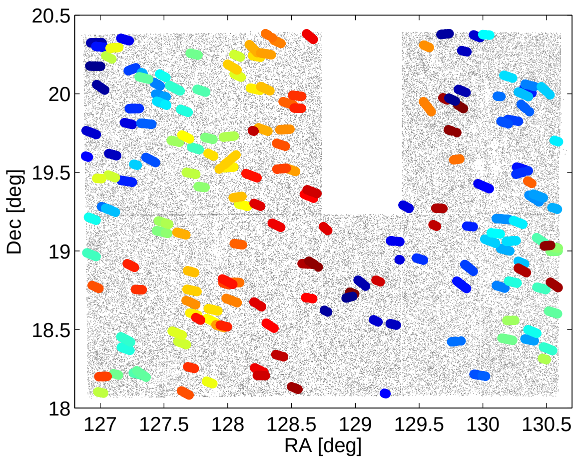

FIG. 1.— A single PTF field of view of 3.6×2.3 deg. The colored circles are the detected asteroids while the grey dots represent stationary background sources. The missing rectangular area is due to a malfunctioning CCD. The data are based on observations of PTF field 110004 taken on Feb 14, 2010 (see Table 1).

multiple nights.

This paper is organized as follows. In §2 we describe the PTF asteroid pipeline. §3 presents the observations analyzed in this study, while in §4 we give the results. Finally we conclude in §5.

2. THE PTF ASTEROID PIPELINE

2.1. *Asteroid identification*

Each PTF image is processed by the IPAC-PTF[11] pipeline. The processing includes splitting the images, de-biasing, flat-fielding, astrometric calibration, preparation of mask images, source extraction and magnitude calibration. An overview of the IPAC-PTF pipeline may be found in Grillmair et al. (2010) and is described in detail by Laher et al. (in prep.). The photometric calibration is discussed in Ofek et al. (2011a). The mask images contain information about bad pixels, probable optical ghosts, saturated pixels, aircraft/satellite tracks and more. The source detection and extraction is performed using SExtractor (Bertin and Arnouts 1996). Here we use the SExtractor MAG_AUTO magnitudes[12] (see Kron 1980). However, our experience is that the MAG_AUTO magnitudes are slightly biased for objects fainter than 19 mag (Ofek et al. 2011a). In the future we plan to use aperture magnitude. The processed images and their associated catalog files are analyzed using the MATLAB-based PTF/Asteroids rotation pipeline described below.

Detection of moving sources is done on a per-field and per-CCD basis in catalog space. For each PTF field/CCD, we construct a reference image based on about ten images with the best seeing values (lowest FWHM and lowest background). Then we use SExtractor to detect the sources in the reference image. We match all the sources with 2″ matching radius in each one of the individual epochs against the reference image catalog. Matching sources against the reference catalog, rather than against one of the epochs, is done for two important reasons: (i) the moving sources do not appear in the reference catalog; and (ii) the deep reference catalogue contains almost all of the stationary sources because faint static sources which are just at, or below, the level of the background noise for a specific image will co-ad to be detected in the reference image. Therefore, even if these stationary sources are detected in only a few of the individual images they will not be mistaken as moving sources.

The sources from each science image that do not appear in the reference catalog are considered as moving source candidates. However, a large fraction of these candidates are cosmic rays, artifacts or spurious detections. A significant part of the artifacts appear in halos around saturated stars and on pixels created by blooming. We identify these sources by their proximity to stars brighter than 11th mag (the Tycho-2 catalog is used as a reference; Høg et al. 2000) and reject them from the list of candidates.

Next, we associate moving source candidates which are detections of the same physical object – we call these "tracks". Tracks are constructed using the following algorithm: for the i-th candidate in the j-th image, the software searches for a second appearance in the $j+1$ image (the images are sorted by time). The search radius is $v_{max}(t_{j+1}-t_j)$, where t_j is the time of the j image and v_{max} is the maximum speed specified by the user[13]. Here, we use $v_{max} = 0.25\,''\mathrm{s}^{-1}$. We note that it is possible to have more than one candidate within the search radius in the $j+1$ image. Therefore, we treat each candidate source in the $j+1$ image as a possible detection of the object in the sequence. For each such possible track we look for another source in the $j+2$ image. The search is done by looking for a source around a position:

$$\alpha_{j+2} = \alpha_{j+1} + \frac{\alpha_{j+1}-\alpha_j}{t_{j+1}-t_j}(t_{j+2}-t_{j+1}), \quad (1)$$

$$\delta_{j+2} = \delta_{j+1} + \frac{\delta_{j+1}-\delta_j}{t_{j+1}-t_j}(t_{j+2}-t_{j+1}). \quad (2)$$

Here α and δ are the right ascension and the declination of the object, respectively, and the subscripts indicate the image index. The search radius, ΔR, around this location is:

$$\Delta R = max(\Delta\alpha_{j+2}, \Delta\delta_{j+2}) + 2'', \quad (3)$$

where

$$\Delta\alpha_{j+2} = \sqrt{\Delta\alpha_{j+1}^2 + \frac{\Delta\alpha_{j+1}^2+\Delta\alpha_j^2}{(t_{j+1}-t_j)^2}(t_{j+2}-t_{j+1})^2}, \quad (4)$$

$$\Delta\delta_{j+2} = \sqrt{\Delta\delta_{j+1}^2 + \frac{\Delta\delta_{j+1}^2+\Delta\delta_j^2}{(t_{j+1}-t_j)^2}(t_{j+2}-t_{j+1})^2}. \quad (5)$$

Here $\Delta\alpha$ and $\Delta\delta$ are the astrometric errors[14] in the right ascension and declination, respectively. 2″ is a constant

[11] Infrared Processing and Analysis Center: http://www.ipac.caltech.edu/

[12] Defined with kron_fact = 1.5 and min_radius = 2.5.

[13] Main belt asteroids have typical angular speeds of $\sim 0.01\,''\mathrm{s}^{-1}$, while near-Earth asteroids can move at a rate of $\sim 0.1\,''\mathrm{s}^{-1}$ and trans-Neptunian objects have a slow motion of order $0.001\,''\mathrm{s}^{-1}$.

[14] The astrometric errors are taken from the square of the SExtractor parameters *ERRX2WIN_IMAGE* and *ERRY2WIN_IMAGE*

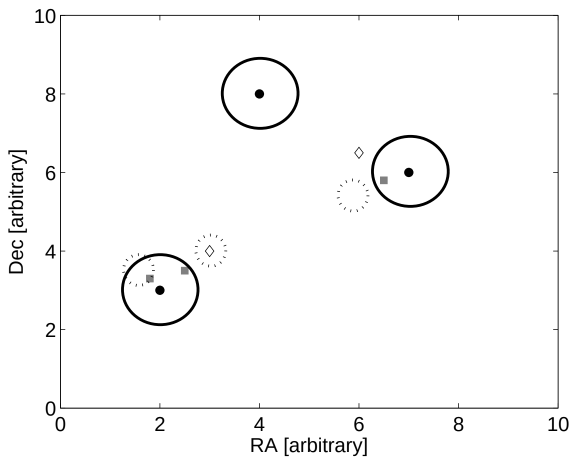

FIG. 2.— Illustration of the track detection algorithm. All symbols are sources that do not appear in the reference image and, therefore, they are treated as moving source candidates. The three black-filled circles appear in the first image. The program searches for candidates in the second image within a radius determined by the user and marked here by empty circles. If a candidate is found in the second image (grey squares), we search for a candidate in the third image (empty diamonds). The search region in the third image (marked by dashed circles) is calculated by Eq. 3. In the case presented here only one asteroid will be detected by the code (i.e., bottom left).

matching radius added in order to avoid problems due to under-estimation of the astrometric errors and any deviations from linear motion of the objects. As a result, moving sources that have a total motion of less than $2''$ in the scanned set of images could not be detected. The search for additional sources associated with each possible track continues recursively on following images, until the moving source does not appear in the $j + n$ image. In case a single source in the first image is branching to multiple possible tracks, our recursive algorithm calculates all the possible tracks and selects the longest track (i.e., the one that contains the greatest number of points) as the most likely track. The sources that belong to this most likely track are flagged as "associated with a track" and the algorithm keeps running on all the sources which are not associated with a track until it runs out of sources or until the sources that remain un-associated cannot be matched. For clarity, the algorithm is visually presented in Figure 2. After scanning all the images, each track is fitted with a second-order polynomial in right ascension and declination using linear least squares, and the χ^2 and degrees of freedom for each fit are stored along with the track's properties.

Since the current version of the algorithm requires an asteroid to appear in successive images, it can identify multiple tracks that, in fact, belong to the same asteroid. This is possible when a moving source is not identified in one of the epochs and this may happen, for example, when the asteroid is blended with a star, or if its signal-to-noise ratio (SNR) is too low in a specific image. Therefore, next we try to merge all the tracks that belong to the same moving object. This is done by fitting the points of any pair of tracks that were observed in the same night, field and CCD to a second order polynomial. Tracks are merged if the χ^2 of the fit is less than a predefined value. Similarly, single "orphan" sources (i.e., sources that do not appear in the reference catalog and were rejected by the detection code in previous steps) are tested as additional points belonging to the detected tracks.

Some of the tracks, especially those containing a small number of points, or those that are very short (i.e., due to small angular speed) may be artifacts and not real astrophysical sources. Another type of false alarm is created by pixels on blooming columns of saturated bright stars that were not flagged by the code in a previous stage and are mistakenly considered as sources by SExtractor. These "objects" have a unique trajectory (i.e., a nearly north-to-south or south-to-north motion) and have similar right ascension values to stars brighter than ~ 11 mag (here also we use the Tycho-2 catalog; Høg et al. 2000). All the unknown detections not marked by the pipeline as false alarms are manually scanned to test their validity. While this manual scan is a simple and fast process, we wish to cancel this step by matching better thresholds to the data and make it completely automatic.

The data collected for each moving source include its position, time, angular velocity (projected into the image data), exposure parameters, χ^2, number of degrees of freedom and instrumental magnitudes measured by SExtractor. Saving these values becomes handy for the remaining steps of the procedure. The detected moving sources are identified by the PyMPChecker webservice[15]. This tool provides asteroid positions around a sky and time coordinates. In addition, all the objects receive an internal PTF designation which is a running number in base 36 (digits + letters). The measured coordinates and photometry are reported to the Minor Planet Center[16].

Asteroids observed on different nights, fields and CCDs are combined into a single track. The identification of different sources as belonging to the same asteroid is done according to the designations of the known objects. If an object is unknown, we fit a second-order polynomial to all the possible track combinations and merge tracks which are consistent with being due to a single moving source. While this method of track merging is limited to data from successive nights, it is sufficient for our purpose of spin analysis.

2.2. *Photometric calibration*

In order to construct the best relative photometry lightcurve of each source we use a linear-least-squares minimization technique, in which we solve for the best zero-point normalization (per epoch), and the best "mean" flux density of each source that minimize the global scatter in all the lightcurves of stationary sources. Furthermore, using a set of linear constraints on the magnitudes of some of the reference stars, we simultaneously calibrate the magnitude to an absolute scale using the r-band magnitude of SDSS stars (York et al. 2000). This technique was introduced by Honeycutt (1992), with some modifications and the simultaneous absolute calibration presented in Ofek et al. (2011b). We note that PTF data routinely achieve relative photometry accuracy of as good as 3 mmag (e.g., van Eyken et al. 2011; Agüeros et al. 2011; Levitan et al. 2011).

[15] http://dotastro.org/PyMPC/PyMPC/
[16] http://minorplanetcenter.net/

We perform the calibration process for each night and each CCD separately. However, some asteroids are visible on multiple nights and/or multiple CCDs. Therefore, the absolute photometric accuracy of SDSS magnitudes (20 mmag) and CCD diversity may introduce a small systematic offset between lightcurves of the same asteroid observed on multiple nights and/or multiple CCDs. We correct for these effects during the period fitting process described in §2.3.

Each moving source is saved with its instrumental magnitude and zero point, for each image. Following the photometric calibration step, the observing times are corrected for light-travel time and the calibrated magnitudes (R_{PTF}) are reduced to geocentric (r) and heliocentric (Δ) distances of 1 AU using:

$$M_{(r=1,\Delta=1)} = R_{PTF} + 5log(r\Delta). \tag{6}$$

The mean calibrated magnitude ($\langle R_{PTF}\rangle$), phase angle (α), geocentric (r) and heliocentric (Δ) distances of the detected asteroids are presented in Tables 2-Table 5. This correction is done only for objects with known orbital parameters.

We do not try to fit the data to a H-G system (i.e., the coefficients that describe the brightness decrease with increasing phase angle), since the phase angles of the observed asteroids change only slightly over the four-day observing period. Instead, we estimate the absolute magnitude H using a fixed G slope of 0.15 and using (Bowell et al. 1989):

$$H = \langle M_{(r=1,\Delta=1)}\rangle + 2.5log[(1-G)\phi_1 + G\phi_2] \tag{7}$$

where

$$\phi_1 = exp(-3.33tan(0.5\langle\alpha\rangle)^{0.63}) \tag{8}$$

$$\phi_2 = exp(-1.87tan(0.5\langle\alpha\rangle)^{1.22}) \tag{9}$$

2.3. *Rotation period analysis*

In order to find the synodic rotation period of the asteroids, we fit a second-order Fourier series to each lightcurve of a merged track:

$$M_j = \sum_{k=1,2}^{N_k} B_k \sin[\frac{2\pi k}{P}(t_j - t_0)] + C_k \cos[\frac{2\pi k}{P}(t_j - t_0)] + \sum_{s=1}^{N_s} Z_s, \tag{10}$$

where B_k and C_k are the Fourier coefficients, P is the rotation period, M_j is the photometric data at t_j (after the reduction to absolute planetary magnitude; i.e., Eq. 6) and t_0 is an arbitrary epoch. As described in §2.2, photometric calibration is performed separately for each set of images taken at different nights and/or CCDs. Therefore, in order to improve the photometric calibration, we also fit in Equation 10 a constant value (Z_s) for each set of images, where a set (s) is defined as all the measurements taken on the same night, field and CCD. N_s is the number of sets. For a given P, this yields a set of linear equations which is solved using least-squares minimization to obtain the free parameters. This calculation is performed for a set of trial frequencies ranging from the Nyquist frequency to one over the total time span of the lightcurve, and in steps of 0.25 divided by the time span of the lightcurve (i.e., over-sampling of 4). The typical trial periods range from about 20 minutes to about 80 hours, which cover the rotation periods of most asteroids (e.g., Pravec and Harris 2000).

The frequency with the minimal χ^2 is chosen as the most likely period. The error in the best-fit frequency is determined by the range of periods with χ^2 smaller than the minimum $\chi^2 + \Delta\chi^2$, where $\Delta\chi^2$ is calculated from the inverse χ^2 distribution assuming $1 + 2N_k + N_s$ degrees of freedom. The code automatically rejects cases in which there are multiple solutions; cases where the best match is at the edge of the tested period range; or if only a few measurements exist (i.e., < 8 data points). All the other matches are manually scanned to test the validity of their period and folded lightcurve. Lightcurves which show two peaks with photometric errors that are smaller than the lightcurve amplitude and features repeating during different nights are considered as good quality lightcurves for which a periodicity can be derived. Poor results include cases where the lightcurve is folded on the photometric noise, giving usually short periods of around 20-30 minutes, which is the approximate sampling rate.

The folded lightcurves receive a reliability code based on the definitions of Warner et al. (2009), which are: '3' for a highly reliable result with full lightcurve coverage; '2' for an ambiguous result based on less than full coverage hence the result may be wrong by an integer ratio; and '1' for periods that are based on fragmentary or noisy lightcurves that may be completely wrong. Only periods with a reliability code of 2 or 3 are used in statistical studies of asteroid rotations. Lightcurves that contain fragmentary data with no repeating features cannot be folded. However, some of these can be used to set lower limits on the rotation periods. These limits are determined from data that show a continuous and convincing magnitude variability (the amplitude is larger than the photometric error) from a single night/CCD set that is the longest in time.

We give lower limits on the amplitude of the lightcurves of all detected asteroids. This amplitude is based on 90% of the magnitude range, Δm, centered on the range median (i.e., rejecting the upper and lower 5% of the data). This is done to avoid photometric measurements which are contaminated by nearby sources or artifacts. Since data from different night/CCD sets might have small differences in their photometric calibration, we calculate the amplitude, A_{min}, separately for each night/CCD set using:

$$A_{min} = \sqrt{\Delta m^2 - \langle\delta m\rangle^2}, \tag{11}$$

where $\langle\delta m\rangle$ is the average photometric error. We list the median value from all the sets as the lower limit on the amplitude. We note that lightcurves with low limits on the amplitudes belong to asteroids that rotate slowly or asteroids with a nearly circular projected shape.

2.4. *Caveats and future improvements*

The current algorithm misses some of the fainter asteroids. This is demonstrated in Figure 3 where the peak of the magnitude distribution of the detected asteroids is at brighter magnitudes than the PTF detection limit. We

are able to find more moving sources, which our search algorithm failed to find, using image blinking. One of the disadvantages of the current algorithm is that, unlike MOPS-like algorithms (e.g., Grav et al. 2011), it is not searching for tracks in all possible combinations of images and that it requires the object to appear in at least three successive images.

This disadvantage is not critical for the main application presented in this paper – rotation period measurements. This is because good photometry is available only for sources which are about one magnitude brighter than the detection limit. Such sources are rarely missed by our algorithm.

3. OBSERVATIONS

We analyze PTF R-band images of four fields observed on four consecutive nights. The PTF field numbers as well as the observing dates are listed in Table 1. The four fields partially overlap (see Figure 4) and cover a total area of 21 deg^2. The footprints of these fields cover ecliptic latitudes between −0.75 deg and +2.5 deg. Table 1 also lists the total number of exposures taken on each night and the time duration of the observing period for acquiring each set of exposures for a given night and field. The seeing in the images ranged between 2.1″ to 2.5″. We note that the observed fields are centered on the open cluster M44, and are also used by Agüeros et al. (2011) to study the mass-period relation of late-K to mid-M stars.

4. RESULTS

4.1. *Detected asteroids*

We use the aforementioned asteroid pipeline to analyze the small set of PTF observations listed in Table 1. Running the algorithm described in §2.1 we found 624 asteroids of which 145 were not yet designated by the Minor Planet Center web service. Figure 4 shows the tracks of all 624 detected asteroids within the field of view. Table 6 lists all of the measurements taken for the 624 objects. The 145 unknown asteroids are fainter than 18.8 mag. The magnitude distribution, presented in Figure 3, shows that more than a third of the asteroids with magnitude between 20 to 21 had not yet been discovered, while most (91%) of the asteroids brighter than 20 are known.

The observed asteroids are located throughout the entire main-belt of asteroids, and spread out to about 4 AU. A few members of the Hungaria group were also detected. Figure 5 presents the diameters[17] of the observed asteroids, estimated assuming a geometric albedo[18] of 0.15, as a function of their semi-major axis (a). The plot shows that the PTF survey can detect asteroids with diameters of hundreds of meters within the inner main-belt (a < 2.5 AU), and 1-km size bodies in the outer main-belt.

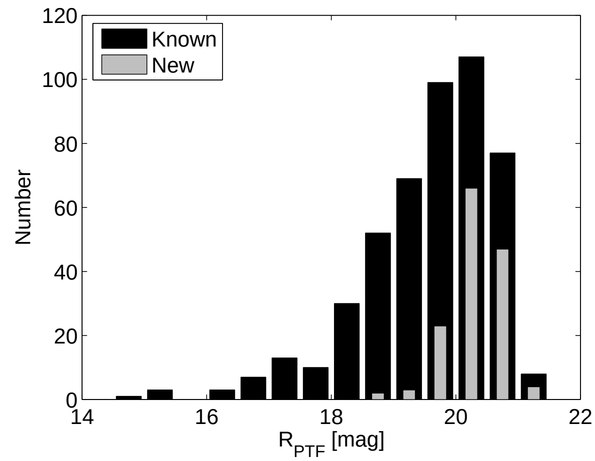

Fig. 3.— The distribution of magnitudes of known (black) and new (grey) asteroids found on this pilot run of the PTF survey. More than one third of the asteroids fainter than 20 mag have not yet been discovered.

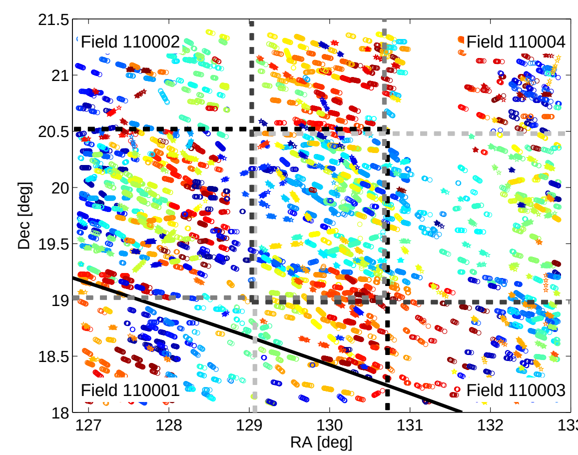

Fig. 4.— The tracks of 624 asteroids detected in the four overlapping fields listed in Table 1 (marked by the dashed lines). Colored circles and pentagons are known and new asteroids, respectively. The black solid line represents the ecliptic.

4.2. *Derived rotation periods*

We were able to derive the rotation periods for 88 asteroids, with high reliability (codes 2 and 3), and, heretofore, none of these have a published lightcurve. The folded lightcurves are presented in Figures 6−9. The lightcurves of 85 objects with possible rotation periods and limits on the rotation period are presented in Figures 10 and 11, respectively. Four of these objects have published spin values, all are larger than the limit on the spin we present here[19]. The rotation periods and amplitudes with high reliability for 88 asteroids are sum-

[17] Diameters are estimated using the formula

$$D = \frac{1329}{\sqrt{Pv}} 10^{-0.2H} \tag{12}$$

where Pv is the geometric albedo and H is the absolute magnitude defined as the brightness of an asteroid at opposition with heliocentric and geocentric distances at 1 AU. The estimated error of the diameters is less than a factor of two, based on a statistical error of 0.12 for G (Lagerkvist & Magnusson 1990) and 0.1 for the albedo.

[18] the geometric albedo in visible light of main belt asteroids ranges from ≈ 0.05 to ≈ 0.4.

[19] These four asteroids with their already published rotation periods are: 1516 Henry - 17.37 h, 6192 1990 KB_1 - 11.1 h (both at *http://obswww.unige.ch/~behrend/page_cou.html*), 10207 Comeniana - 12.84 h (Galad et al. 2009), 23971 1998 YU_9 - 6.8949 h (*http://www.asu.cas.cz/~ppravec/neo.htm*).

TABLE 1
OBSERVED FIELDS

FIELD ID	RA [deg]	Dec [deg]	Feb12 N_{exp}, Δt	Feb13 N_{exp}, Δt	Feb14 N_{exp}, Δt	Feb15 N_{exp}, Δt
110001	128.75	+19.25	23, 6.87	20, 8.57	29, 8.65	29, 8.70
110002	128.75	+20.24	23, 6.87	19, 8.58	29, 8.65	29, 8.74
110003	131.00	+19.25	23, 6.87	20, 8.88	29, 8.69	29, 8.74
110004	131.00	+20.24	23, 6.87	20, 8.88	29, 8.69	28, 8.78

NOTE. — FIELD ID is a unique number representing PTF fields. N_{exp} is the number of exposures per night and field, and Δt is the duration of time spanned by each set of observations, in hours. All observations were taken on 2010

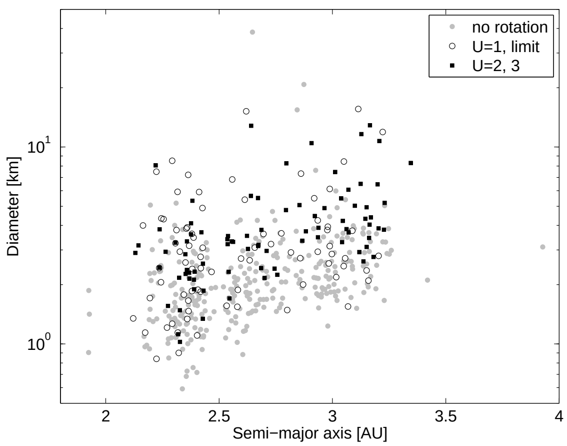

FIG. 5.— The estimated diameters of the known observed asteroids as a function of their semi-major axis (a). Main-belt asteroids as small as 600 m are seen in this sample. A few bodies from the Hungaria group can be seen at $a < 2\,AU$. The gap at $a = 2.5\,AU$ is the 1:3 Kirkwood gap.

marized in Table 2. The possible rotation periods of 18 asteroids are shown in Table 3, while the lower limits on the rotation periods of 67 asteroids are listed in Table 4. We also provide lower limits on the amplitude of the rest of the detected asteroids in Table 5.

Since most of the asteroids were observed during all four nights, where the total time span between the first and the last images taken was about 80 hours, this gives us an opportunity to detect rotations as slow as tens of hours. Since the field of view was observed during the entire night over the course of four consecutive nights, most asteroids in our survey were observed for a total of about 32 hours (Table 1). Some of the asteroids were observed for shorter times due to poor weather conditions (especially on February 12) or because they were not within the field footprints in all four nights.

Among the lightcurves, three have features that are common among binary asteroids (Pravec et al. 2006). These features are deep V-shaped minima and wide inverted-U-shaped maxima. The deep V-shaped minima presumably represent a mutual event of eclipse or occultation between the primary and the secondary components. The three asteroids associated with the three aforementioned lightcurves are (17293) 2743 P-L (Figure 10); (101668) 1999 CR_{95} (Figure 8) and (231927) 2001 DU_{30} (Figure 9). We note that there are some inconsistencies in the shape of the lightcurve of (17293) 2743 P-L as seen on different nights. If our estimated period is valid, then this may be the result of a non-spherical shape of one of the rotating components imposed on the brightness attenuation from the mutual event. The binary nature of these three objects should be confirmed with follow-up observations. If the features in these lightcurves are indeed due to mutual events of binary asteroids, then the periods reported here are the orbital periods of the components about their center of mass, and the minima depth represents the approximate ratio between the diameters of the components.

5. SUMMARY AND FUTURE PROSPECTS

We present a pipeline that finds asteroids, constructs their lightcurves, and measures their rotation periods using images acquired by the PTF survey. We demonstrate our pipeline performance using a small sample of PTF data consisting of observations of about 21 deg^2 obtained over four nights with a cadence of $\sim$ 20 min. Within these images, we find 624 asteroids, of which 145 ($\cong$ 20%) were previously unknown. This shows that PTF is an efficient survey for studying known, as well as unknown asteroids. Among the new discoveries, many are small, km-sized, objects. These may reveal the orbits of physically interesting objects such as small members of dynamical families (Bendjoya & Zappalá 2002) and secondary members of rotationally-disintegrated objects (known as *asteroid pairs*; Vokrouhlický & Nesvorný 2008).

We obtain from our analysis high quality rotation periods for 88 main-belt asteroids and additional possible periods for 85 other asteroids. Based on the ecliptic latitude distribution of PTF high-cadence observations and our success rate in measuring asteroid periodicities, we roughly estimate that PTF can measure the rotation periods for about 10,000 asteroids. This large sample could be used to study the effects of different physical mechanisms on the spin evolution of asteroids. These mechanisms, such as collisions, the thermal YORP effect and tidal forces that follow planetary encounters, leave different signatures on the spin distribution of asteroids. For example, collisions generate a Maxwellian spin-rate distribution, as can be seen for large asteroids (>40 km; Pravec and Harris 2000), while the YORP effect creates a flatter spin-rate distribution (Pravec et al. 2008). A large PTF sample of asteroid rotation periods also could be used to compare the rotations of asteroids in different size groups and dynamical families (e.g., Polishook and Brosch 2009), and to track the rotational history of components ejected from rotationally-disintegrated asteroids (Pravec et al. 2010).

Dust and gas ejection from minor planets can be the result of cometary activity or a collisional event. Such

objects can be detected as moving sources, with a signature extended point-spread function. The large sample of asteroids visible in PTF images is being used to search for gas and dust around minor planets and to probe their ice content, as well as to study the dynamical history of the main belt (Waszczak, Ofek & Polishook 2011; Waszczak et al., in prep.).

PTF photometry is calibrated to a precision of better than 0.04 magnitudes, even outside SDSS footprints (Ofek et al. 2011a) and it provides accurate magnitudes of asteroids in the visible range. Therefore, PTF data could be combined with the archive of NASA's Wide-field Infrared Survey Explorer (WISE) telescope. During nine months of full cryogenic operations, the WISE telescope observed about 200,000 asteroids in the near-IR (Mainzer et al. 2010); most of these lack accurate absolute magnitudes in visible wavelengths (Masiero et al. 2011). Therefore, the two data sets combined could improve the size measurements for a significant number of asteroids.

Binary asteroids are difficult to identify because eclipses/occultations repeat themselves only after long periods (tens of hours) and last for short times. Our survey can find a large number of binary asteroids through the detection of eclipses and occultations. This can provide the statistics on binary asteroids as a function of their physical parameters. It is estimated that approximately 16% of near-Earth asteroids are binaries (Margot et al. 2002). Applying this ratio to main-belt asteroids, and assuming that eclipses/occultations can be detected during 10% to 30% of the orbital period (Pravec et al. 2006), it can be estimated that out of ≈ 100 asteroids measured photometrically by the PTF, between 2 and 5 objects will register an eclipse or an occultation. This ratio is supported by our findings of three binary candidates. Enlarging the sample could determine the number of binaries among main-belt asteroids. This has important implications because any difference between the fraction of binaries among main-belt asteroids and near-Earth asteroids can constrain binary formation mechanisms and their dependencies on the asteroid environment.

The photometry of asteroids measured by PTF could also be used to derive asteroid shapes and rotational states (sidereal period and spin axis). This is done by the lightcurve inversion method that uses brightness measurements obtained over a wide range of viewing geometries during a few apparitions to build a complete model of the asteroid (e.g., Kaasalainen and Torppa 2001, Hanuš et al. 2011). PTF will revisit many asteroids during a few apparitions, and so the lightcurve inversion method could be applied to a large sample of small-sized asteroids, thus contributing to the study of asteroid spins and shapes.

We thank the referee for useful comments. This paper is based on observations obtained with the Samuel Oschin Telescope as part of the Palomar Transient Factory project, a scientific collaboration between the California Institute of Technology, Columbia University, Las Cumbres Observatory, the Lawrence Berkeley National Laboratory, the National Energy Research Scientific Computing Center, the University of Oxford, and the Weizmann Institute of Science. The Weizmann PTF partnership is funded in part by grants from the Israeli Science Foundation (ISF) to AG. PTF Collaborative work between the Weizmann and Caltech groups is supported by the Binational Science Foundation (BSF) via grants to SRK and AG. D Polishook further acknowledges support from the Benoziyo Center for Astrophysics and the Yeda-Sela Center at WIS. SRK and his group are partially supported by the NSF grant AST–0507734. SBC wishes to acknowledge generous support from Gary and Cynthia Bengier, the Richard and Rhoda Goldman Fund, NASA/*Swift* grant NNX10AI21G, NASA/*Fermi* grant NNX1OA057G, and National Science Foundation (NSF) grant AST–0908886.

REFERENCES

Agüeros, M. A., Covey, K. R., Lemonias, J. J., et al. 2011, ApJ, 740, 110
Arcavi, I., Gal-Yam, A., Kasliwal, M. M., et al. 2010, ApJ, 721, 777
Bendjoya, P., & Zappalà, V. 2002, Asteroids III, 613
Bertin, E., & Arnouts, S. 1996, A&AS, 117, 393
Bowell, E., Hapke, B., Domingue, D., et al. 1989, Asteroids II, 524
Davis, D. R., Durda, D. D., Marzari, F., Campo Bagatin, A., & Gil-Hutton, R. 2002, Asteroids III, 545
Galad, A., Kornos, L., & Gajdos, S. 2009, Minor Planet Bulletin, 36, 13
Gnat, O., & Sari, R. 2010, ApJ, 719, 1602
Grav, T., Jedicke, R., Denneau, L., et al. 2011, PASP, 123, 423
Grillmair, C. J., Laher, R., Surace, J., et al. 2010, Astronomical Data Analysis Software and Systems XIX, 434, 28
Hanuš, J., Ďurech, J., Brož, M., et al. 2011, A&A, 530, A134
Harris, A. W., Young, J. W., Bowell, E., et al. 1989, Icarus, 77, 171
Høg, E., Fabricius, C., Makarov, V. V., et al. 2000, A&A, 355, L27
Honeycutt, R. K. 1992, PASP, 104, 435
Ivezić, Ž., Tabachnik, S., Rafikov, R., et al. 2001, AJ, 122, 2749
Kaasalainen, M., & Torppa, J. 2001, Icarus, 153, 24
Kron, R. G. 1980, ApJS, 43, 305
Lagerkvist, C.-I., & Magnusson, P. 1990, A&AS, 86, 119
Laher, et al. 2011, In prep.
Law, N. M., Kulkarni, S. R., Dekany, R. G., et al. 2009, PASP, 121, 1395
Levitan, D., Fulton, B. J., Groot, P. J., et al. 2011, ApJ, 739, 68
Mainzer, A. K., Wright, E. L., Bauer, J. M., et al. 2010, Bulletin of the American Astronomical Society, 42, 1016
Margot, J. L., Nolan, M. C., Benner, L. A. M., et al. 2002, Science, 296, 1445
Masiero, J., Jedicke, R., Ďurech, J., et al. 2009, Icarus, 204, 145
Masiero, J. R., Mainzer, A. K., Grav, T., et al. 2011, ApJ, 741, 68
Ofek, E. O. 2011, arXiv:xxxx.xxxx, submitted to ApJ
Ofek, E. O., Laher, R., Law, N., et al. 2011a, arXiv:1112.4851
Ofek, E. O., Frail, D. A., Breslauer, B., et al. 2011b, ApJ, 740, 65
Polishook, D., & Brosch, N. 2009, Icarus, 199, 319
Polishook, D., Brosch, N., & Prialnik, D. 2011, Icarus, 212, 167
Pravec, P., & Harris, A. W. 2000, Icarus, 148, 12
Pravec, P., Scheirich, P., Kušnirák, P., et al. 2006, Icarus, 181, 63
Pravec, P., Harris, A. W., Vokrouhlický, D., et al. 2008, Icarus, 197, 497
Pravec, P., Vokrouhlický, D., Polishook, D., et al. 2010, Nature, 466, 1085
Rahmer, G., Smith, R., Velur, V., et al. 2008, Proc. SPIE, 7014,
Rau, A., Kulkarni, S. R., Law, N. M., et al. 2009, PASP, 121, 1334
Rubincam, D. P. 2000, Icarus, 148, 2
van Eyken, J. C., Ciardi, D. R., Rebull, L. M., et al. 2011, AJ, 142, 60
Vokrouhlický, D., & Čapek, D. 2002, Icarus, 159, 449
Vokrouhlický, D., & Nesvorný, D. 2008, AJ, 136, 280
Warner, B. D., Harris, A. W., & Pravec, P. 2009, Icarus, 202, 134
Waszczak, A., Ofek, E. O., & Polishook, D. 2011, Central Bureau Electronic Telegrams, 2823, 1
Waszczak, A., et al. 2011, in prep
York, D. G., Adelman, J., Anderson, J. E., Jr., et al. 2000, AJ, 120, 1579

TABLE 2
Synodic rotation periods of 88 asteroids with high reliability

Designation	N_{nights}	N_{im}	r [AU]	Δ [AU]	α [deg]	Period [hour]	U	Amp [mag]	$\langle R_{PTF} \rangle$ [mag]	a [AU]
(2960) Ohtaki	2	57	2	1.03	8.1	5.31 ± 0.03	3	$\gtrsim 0.37$	15.42 ± 0.02	2.22
(3597) Kakkuri	4	97	3.23	2.28	5.6	27 ± 0.5	2	$\gtrsim 0.58$	16.78 ± 0.03	3.17
(5217) Chaozhou	1	20	2.3	1.33	7.1	11.3 ± 0.6	2	$\gtrsim 0.56$	16.73 ± 0.01	2.38
(6262) Javid	3	155	3.01	2.05	5.7	8.02 ± 0.05	3	$\gtrsim 0.45$	17.11 ± 0.03	2.91
(7270) Punkin	4	56	3.79	2.84	4.8	7.51 ± 0.07	3	$\gtrsim 0.5$	18.25 ± 0.04	3.21
(7728) Giblin	2	27	3.02	2.06	5.1	11.8 ± 0.3	2	$\gtrsim 0.61$	17.18 ± 0.02	2.8
(8120) Kobe	3	79	2.76	1.81	6.8	5.86 ± 0.04	3	$\gtrsim 0.74$	18.8 ± 0.05	2.42
(8128) Nicomachus	2	74	3.13	2.17	5.3	4.67 ± 0.02	3	$\gtrsim 0.54$	17.19 ± 0.03	3.13
(9921) 1981 EO18	3	55	2.33	1.36	6.2	8.01 ± 0.03	3	$\gtrsim 0.33$	17.37 ± 0.02	2.38
(10121) Arzamas	4	192	3.67	2.72	4.7	12.1 ± 0.3	3	$\gtrsim 0.66$	18.87 ± 0.05	3.2
(11705) 1998 GN7	1	20	2.99	2.03	5.3	3.8 ± 0.3	2	$\gtrsim 0.32$	16.65 ± 0.02	2.64
(12845) Crick	3	86	2.81	1.86	6.6	3.52 ± 0.05	2	$\gtrsim 0.21$	18.51 ± 0.04	2.79
(12895) Balbastre	3	128	2.03	1.07	8.7	3.8 ± 0.04	2	$\gtrsim 0.32$	17.02 ± 0.02	2.24
(13246) 1998 MJ33	4	222	2.53	1.57	6.9	14 ± 0.2	3	$\gtrsim 0.25$	17.48 ± 0.03	2.67
(14164) Hennigar	2	49	2.82	1.86	6.2	11.8 ± 0.2	2	$\gtrsim 0.88$	18.54 ± 0.04	2.94
(14197) 1998 XK72	4	161	3.02	2.06	5.7	10.7 ± 0.1	3	$\gtrsim 0.67$	18.17 ± 0.04	3.04
(14712) 2000 CO51	3	36	3.18	2.23	5.6	13.7 ± 0.2	2	$\gtrsim 0.42$	17.83 ± 0.03	3.01
(16228) 2000 EC39	4	123	3.6	2.65	5.3	6.2 ± 0.2	2	$\gtrsim 0.27$	19.17 ± 0.06	3.12
(20601) 1999 RD197	3	59	3.41	2.47	5.6	3.36 ± 0.04	3	$\gtrsim 0.24$	19.02 ± 0.05	2.64
(21705) Subinmin	3	65	2.87	1.91	5.6	3.46 ± 0.03	3	$\gtrsim 0.62$	18.91 ± 0.06	2.69
(25112) Mymeshkovych	3	76	2.94	1.98	5.7	10.1 ± 0.2	2	$\gtrsim 0.44$	19.06 ± 0.06	2.88
(25171) 1998 SX66	3	97	3.03	2.07	5.6	11.6 ± 0.2	3	$\gtrsim 0.5$	18.99 ± 0.06	2.92
(28509) 2000 CB92	2	23	2.27	1.3	6.9	5.04 ± 0.09	2	$\gtrsim 0.43$	18.28 ± 0.03	2.26
(32522) 2001 OE81	3	30	2.49	1.53	7.5	3.62 ± 0.01	3	$\gtrsim 0.26$	18.2 ± 0.03	2.38
(32553) 2001 QC27	3	30	3.53	2.57	4.3	4 ± 0.05	3	$\gtrsim 0.26$	18.35 ± 0.05	3.35
(33934) 2000 LA30	3	54	2.92	1.97	6.1	5.2 ± 0.1	2	$\gtrsim 0.67$	20.2 ± 0.1	2.39
(35005) 1979 MY3	4	72	2.83	1.88	6.6	7.24 ± 0.06	2	$\gtrsim 0.47$	19.27 ± 0.06	2.56
(36349) 2000 NZ23	4	104	2.73	1.77	6.7	6.7 ± 0.1	3	$\gtrsim 0.43$	19.01 ± 0.05	2.54
(36402) 2000 OT47	4	110	2.79	1.83	6.5	8.2 ± 0.05	3	$\gtrsim 0.57$	18.93 ± 0.05	2.54
(36524) 2000 QS80	3	81	2.5	1.54	7.1	4.26 ± 0.03	3	$\gtrsim 0.44$	18.32 ± 0.03	2.56
(44534) 1998 YZ9	4	144	2.16	1.21	9	22.5 ± 0.5	2	$\gtrsim 0.7$	18.61 ± 0.04	2.37
(45259) 2000 AF1	3	56	3.25	2.3	6.1	11.7 ± 0.2	3	$\gtrsim 0.85$	19.54 ± 0.07	2.94
(45601) 2000 DE5	3	33	3.08	2.12	4.9	3.38 ± 0.01	3	$\gtrsim 0.32$	18.63 ± 0.05	2.96
(46672) 1996 OA	2	37	3.33	2.37	5.3	3.55 ± 0.02	3	$\gtrsim 0.4$	19.08 ± 0.05	3.1
(47149) 1999 RX34	4	100	2.52	1.56	7	9.5 ± 0.09	3	$\gtrsim 0.49$	18.55 ± 0.04	2.13
(47154) 1999 RE141	3	64	2.89	1.94	6.1	5.2 ± 0.02	3	$\gtrsim 0.67$	19.71 ± 0.08	2.69
(48233) 2001 LY9	3	79	3.56	2.61	5.3	3.62 ± 0.02	3	$\gtrsim 0.7$	19.52 ± 0.07	3.17
(49766) 1999 WS	2	24	2.34	1.39	7.9	6.7 ± 0.1	2	$\gtrsim 0.76$	18.5 ± 0.04	2.14
(57394) 2001 RD84	4	52	2.21	1.24	7	6.74 ± 0.06	3	$\gtrsim 0.6$	18.29 ± 0.06	2.32
(57815) 2001 WV25	2	30	2.5	1.55	7.2	6 ± 0.08	2	$\gtrsim 0.34$	18.79 ± 0.04	2.35
(60527) 2000 EE43	3	59	2.97	2.02	6.5	6.01 ± 0.04	2	$\gtrsim 0.36$	19.08 ± 0.05	3.05
(61358) 2000 PK12	4	113	2.74	1.78	6.1	2.57 ± 0.02	2	$\gtrsim 0.28$	19.01 ± 0.05	2.54
(61378) 2000 PU28	3	103	2.88	1.92	6.2	4.69 ± 0.01	3	$\gtrsim 0.79$	19.84 ± 0.09	2.43
(63429) 2001 MH5	2	34	2.67	1.72	7.2	9.2 ± 0.2	3	$\gtrsim 0.78$	19.29 ± 0.06	2.31
(69802) 1998 RX15	2	18	3.01	2.05	5.8	5.3 ± 0.1	2	$\gtrsim 0.48$	19.47 ± 0.07	2.87
(71314) 2000 AW76	2	56	2.81	1.86	6.5	5.65 ± 0.08	3	$\gtrsim 0.81$	18.45 ± 0.05	2.85
(74421) 1999 AW24	3	58	2.86	1.91	6.7	3.66 ± 0.02	3	$\gtrsim 0.42$	18.98 ± 0.05	3.16
(77768) 2001 QM	3	36	3.2	2.24	4.6	7.1 ± 0.2	2	$\gtrsim 0.34$	18.77 ± 0.07	3.23
(77829) 2001 QO217	3	125	3.09	2.14	5.5	13.6 ± 0.3	3	$\gtrsim 0.62$	18.86 ± 0.06	3.2
(78296) 2002 PT53	2	23	3.14	2.18	5.3	5.3 ± 0.1	3	$\gtrsim 0.94$	19.22 ± 0.07	3.07
(78420) 2002 QU40	2	22	3.44	2.48	4.5	4.9 ± 0.05	2	$\gtrsim 1.11$	19.33 ± 0.07	3.07
(79721) 1998 SE112	3	44	2.84	1.89	6.7	10.2 ± 0.6	2	$\gtrsim 0.45$	20.2 ± 0.1	2.24
(87028) 2000 JA78	3	93	2.76	1.81	6.2	6.02 ± 0.09	2	$\gtrsim 0.57$	19.77 ± 0.08	2.35
(87988) 2000 TZ62	2	32	2.25	1.28	6.6	4.1 ± 0.2	2	$\gtrsim 0.42$	17.92 ± 0.05	2.62
(90896) 1997 CJ3	3	91	2.44	1.48	7.8	7.4 ± 0.2	2	$\gtrsim 0.45$	18.36 ± 0.04	2.67
(92519) 2000 NO27	4	186	2.46	1.5	6.8	3.08 ± 0.02	3	$\gtrsim 0.26$	18.48 ± 0.05	2.36
(93335) 2000 SK235	3	65	2.42	1.47	7.5	6.3 ± 0.1	3	$\gtrsim 0.9$	20 ± 0.1	2.55
(94653) 2001 WF67	3	92	2.13	1.18	9.4	4.8 ± 0.06	3	$\gtrsim 0.73$	19.17 ± 0.06	2.39
(95796) 2003 FM24	2	30	2.54	1.58	6.1	7.2 ± 0.2	2	$\gtrsim 0.45$	19.62 ± 0.08	2.39
(98993) 2001 DC36	2	46	2.75	1.79	6.4	3.22 ± 0.03	2	$\gtrsim 0.58$	19.6 ± 0.07	2.74
(101668) 1999 CR95[a]	4	178	2.82	1.87	6.1	16.54 ± 0.06	2	$\gtrsim 0.81$	18.79 ± 0.05	3.15
(105026) 2000 KX30	4	109	3.24	2.28	5	4.25 ± 0.02	3	$\gtrsim 0.73$	19.68 ± 0.08	3.16
(116449) 2004 AU	4	124	2.61	1.65	6.5	15.3 ± 0.7	2	$\gtrsim 0.33$	18.24 ± 0.04	3.15
(118217) 1996 EO7	2	28	1.99	1.03	8.8	5.61 ± 0.09	2	$\gtrsim 1.06$	19.27 ± 0.06	2.33
(121532) 1999 UD40	2	20	2.88	1.92	5.7	2.25 ± 0.01	2	$\gtrsim 0.5$	19.48 ± 0.08	2.67
(124260) 2001 QK12	3	190	2.49	1.53	7	2.75 ± 0.01	2	$\gtrsim 0.62$	19.73 ± 0.08	2.37
(124374) 2001 QU152	2	51	2.26	1.3	8.1	9.7 ± 0.3	2	$\gtrsim 0.61$	19.33 ± 0.06	2.27
(124966) 2001 TH105	3	51	2.31	1.36	8.3	5.5 ± 0.04	2	$\gtrsim 0.65$	19.11 ± 0.05	2.43
(126334) 2002 AW152	4	53	2.42	1.47	7.7	3.51 ± 0.02	2	$\gtrsim 0.43$	19.26 ± 0.06	2.54
(126935) 2002 EN146	3	116	2.83	1.88	6.3	6.03 ± 0.05	3	$\gtrsim 0.88$	19.7 ± 0.08	2.63
(129100) 2004 XY4	2	57	2.65	1.69	6.5	6.8 ± 0.1	3	$\gtrsim 0.97$	19.51 ± 0.07	2.71

Note. — Columns: asteroids' designations, number of nights, number of images, geocentric (r) and heliocentric (Δ) distances, phase angle (α), rotation periods, period's reliability code, lightcurve amplitude, mean magnitude, semi-major axis.

[a] A possible binary asteroid. The period is probably the orbital period of the satellite.

TABLE 2
CONTINUED

Designation	N_{nights}	N_{im}	r [AU]	Δ [AU]	α [deg]	Period [hour]	U	Amp [mag]	$\langle R_{PTF} \rangle$ [mag]	a [AU]
(192591) 1999 CE8	3	59	2.59	1.64	7.8	4.59 ± 0.03	3	$\gtrsim 0.36$	18.83 ± 0.04	3.15
(192665) 1999 RS181	3	73	2.69	1.73	6.4	5.45 ± 0.05	2	$\gtrsim 0.74$	20.2 ± 0.1	2.7
(195812) 2002 QL19	3	36	3.33	2.37	4.5	4.66 ± 0.03	3	$\gtrsim 0.71$	19.99 ± 0.1	3.04
(196214) 2003 BD37	2	36	2.34	1.38	7.5	6.8 ± 0.1	2	$\gtrsim 0.55$	19.16 ± 0.06	2.36
(197402) 2003 YN34	2	22	2.71	1.76	7.1	3.9 ± 0.02	2	$\gtrsim 0.93$	19.71 ± 0.08	3.14
(215701) 2003 YD121	3	49	3.31	2.35	4.4	6 ± 0.1	2	$\gtrsim 0.6$	19.71 ± 0.08	3.23
(230204) 2001 ST265	2	28	2.16	1.2	8.4	4.6 ± 0.1	2	$\gtrsim 0.66$	20.2 ± 0.1	2.43
(231051) 2005 GW60	2	29	3.3	2.36	5.8	9.4 ± 0.8	2	$\gtrsim 0.67$	20.2 ± 0.1	3.18
(231717) 1999 CK9	2	36	2.66	1.7	6.5	4.2 ± 0.1	2	$\gtrsim 0.57$	19.39 ± 0.07	3.12
(231927) 2001 DU30[a]	4	177	2.19	1.23	7.9	24.4 ± 0.1	2	$\gtrsim 0.72$	18.62 ± 0.05	2.76
(231958) 2001 PF28	2	46	2.89	1.93	5.6	4.5 ± 0.1	2	$\gtrsim 0.6$	19.11 ± 0.06	3.06
(283741) 2002 XH118	3	55	2.14	1.18	8.9	6.48 ± 0.02	3	$\gtrsim 1.09$	20.1 ± 0.1	2.33
2010 CA149	3	93	1.98	1.02	9.2	5.04 ± 0.03	2	$\gtrsim 0.71$	19.76 ± 0.09	2.32
2010 CV249	2	35	···	···	···	5.9 ± 0.2	2	$\gtrsim 0.51$	20.5 ± 0.1	3.26
P0007F	2	56	···	···	···	7.4 ± 0.3	2	$\gtrsim 0.93$	20.3 ± 0.1	···
P00095	2	39	···	···	···	3.26 ± 0.03	2	$\gtrsim 0.83$	20.6 ± 0.1	···
P000ZL	2	53	···	···	···	6.7 ± 0.2	2	$\gtrsim 0.73$	20.05 ± 0.1	···

[a] A possible binary asteroid. The period is probably the orbital period of the satellite.

TABLE 3
UNCERTAIN SYNODIC ROTATION PERIODS (U=1) OF 18 ASTEROIDS

Designation	N_{nights}	N_{im}	r [AU]	Δ [AU]	α [deg]	Period [hour]	U	Amp [mag]	$\langle R_{PTF} \rangle$ [mag]	a [AU]
(9337) 1991 FO1	1	52	2.8	1.84	5.6	3.2 ± 0.1	1	$\gtrsim 0.26$	17.46 ± 0.02	2.86
(11027) Astaf'ev	4	106	2.32	1.37	8.4	4.87 ± 0.07	1	$\gtrsim 0.18$	17.75 ± 0.03	2.16
(13503) 1988 RH6	3	92	2.37	1.41	8.1	6.9 ± 0.1	1	$\gtrsim 0.23$	17.65 ± 0.03	2.25
(17293) 2743 P-L[a]	3	115	2.11	1.16	9.3	23.24 ± 0.07	1	$\gtrsim 0.43$	17.53 ± 0.02	2.39
(30338) 2000 JW29	4	145	2.15	1.19	8.2	39 ± 1	1	$\gtrsim 0.44$	17.82 ± 0.03	2.31
(31388) 1998 YL2	2	22	2.17	1.2	7.2	4.27 ± 0.03	1	$\gtrsim 0.3$	18.41 ± 0.04	2.38
(40791) 1999 TO33	3	64	2.82	1.87	6.8	3.133 ± 0.008	1	$\gtrsim 0.66$	19.09 ± 0.05	2.7
(47714) 2000 DS24	1	34	3.33	2.38	5.8	10 ± 2	1	$\gtrsim 0.57$	19.64 ± 0.07	2.98
(56682) 2000 LA9	3	125	2.22	1.26	7.8	2.54 ± 0.04	1	$\gtrsim 0.15$	18.05 ± 0.05	2.33
(113117) 2002 RF80	2	24	2.76	1.81	6.4	12.3 ± 0.2	1	$\gtrsim 0.72$	19.3 ± 0.07	3.2
(115359) 2003 SA250	1	36	3.03	2.09	6.4	5.4 ± 0.08	1	$\gtrsim 1.46$	19.6 ± 0.08	2.94
(129691) 1998 SH16	3	86	2.91	1.96	5.9	17.1 ± 0.8	1	$\gtrsim 0.62$	20.4 ± 0.1	2.87
(133528) Ceragioli	3	79	3.02	2.08	6.6	3.06 ± 0.04	1	$\gtrsim 0.52$	20.1 ± 0.1	2.86
(197388) 2003 YN11	3	108	2.98	2.02	5.8	14.9 ± 0.9	1	$\gtrsim 0.83$	20.2 ± 0.1	3.15
(228255) 1999 ET7	3	45	2.88	1.93	6.2	4.2 ± 0.1	1	$\gtrsim 0.54$	20.3 ± 0.1	3.16
2003 WP9	3	98	2.9	1.94	6	6.76 ± 0.05	1	$\gtrsim 0.83$	20.2 ± 0.1	3.02
2007 EZ184	3	54	···	···	···	2 ± 0.03	1	$\gtrsim 0.52$	20.3 ± 0.1	2.27
P000K7	2	44	···	···	···	3.23 ± 0.02	1	$\gtrsim 0.47$	19.4 ± 0.06	···

NOTE. — Columns like Table 2.
[a] A possible binary asteroid. The period is probably the orbital period of the satellite.

TABLE 4
LOWER LIMITS ON THE SYNODIC ROTATION PERIODS OF 67 ASTEROIDS

Designation	N_{nights}	N_{im}	r [AU]	Δ [AU]	α [deg]	Period [hour]	Amp [mag]	$\langle R_{PTF} \rangle$ [mag]	a [AU]
(1516) Henry	2	23	2.48	1.51	6.3	$\gtrsim 5$	$\gtrsim 0.03$	15.13 ± 0.02	2.62
(1788) Kiess	2	37	3.61	2.65	4.9	$\gtrsim 9$	$\gtrsim 0.8$	17.29 ± 0.03	3.11
(3111) Misuzu	1	38	2.29	1.33	7.2	$\gtrsim 9$	$\gtrsim 0.18$	16.47 ± 0.02	2.22
(4741) Leskov	3	46	3.68	2.74	5.2	$\gtrsim 9$	$\gtrsim 0.1$	17.85 ± 0.03	3.22
(5807) Mshatka	3	49	3.37	2.42	5.4	$\gtrsim 8.6$	$\gtrsim 0.3$	18.06 ± 0.04	3.05

NOTE. — Columns: asteroids' designations, number of nights, number of images, geocentric (r) and heliocentric (Δ) distances, phase angle (α), limit on the rotation period, lightcurve amplitude, mean magnitude, semi-major axis. This table is published in its entirety in the electronic edition of *MNRAS*. A portion of the full table is shown here for guidance regarding its form and content.

TABLE 5
Lower limits on the amplitude of 451 asteroids

Designation	N_{nights}	N_{im}	r [AU]	Δ [AU]	α [deg]	Amp [mag]	$\langle R_{PTF} \rangle$ [mag]	a [AU]
(625) Xenia	3	57	3.2	2.25	5.8	$\gtrsim 0$	14.49 ± 0.02	2.65
(1079) Mimosa	2	14	2.8	1.84	5.77	$\gtrsim 0.1$	14.95 ± 0.04	2.87
(3679) Condruses	2	23	2.34	1.38	7.65	$\gtrsim 0.1$	15.13 ± 0.02	2.2
(5179) Takeshima	2	37	2.22	1.26	7.21	$\gtrsim 0.1$	17.29 ± 0.03	2.31
(6916) Lewispearce	2	57	3.2	2.25	5.34	$\gtrsim 0.3$	15.42 ± 0.02	2.84

Note. — Columns: asteroids' designations, number of nights, number of images, geocentric (r) and heliocentric (Δ) distances, phase angle (α), lower limit on the lightcurve amplitude, mean magnitude, semi-major axis. This table is published in its entirety in the electronic edition of *MNRAS*. A portion of the full table is shown here for guidance regarding its form and content.

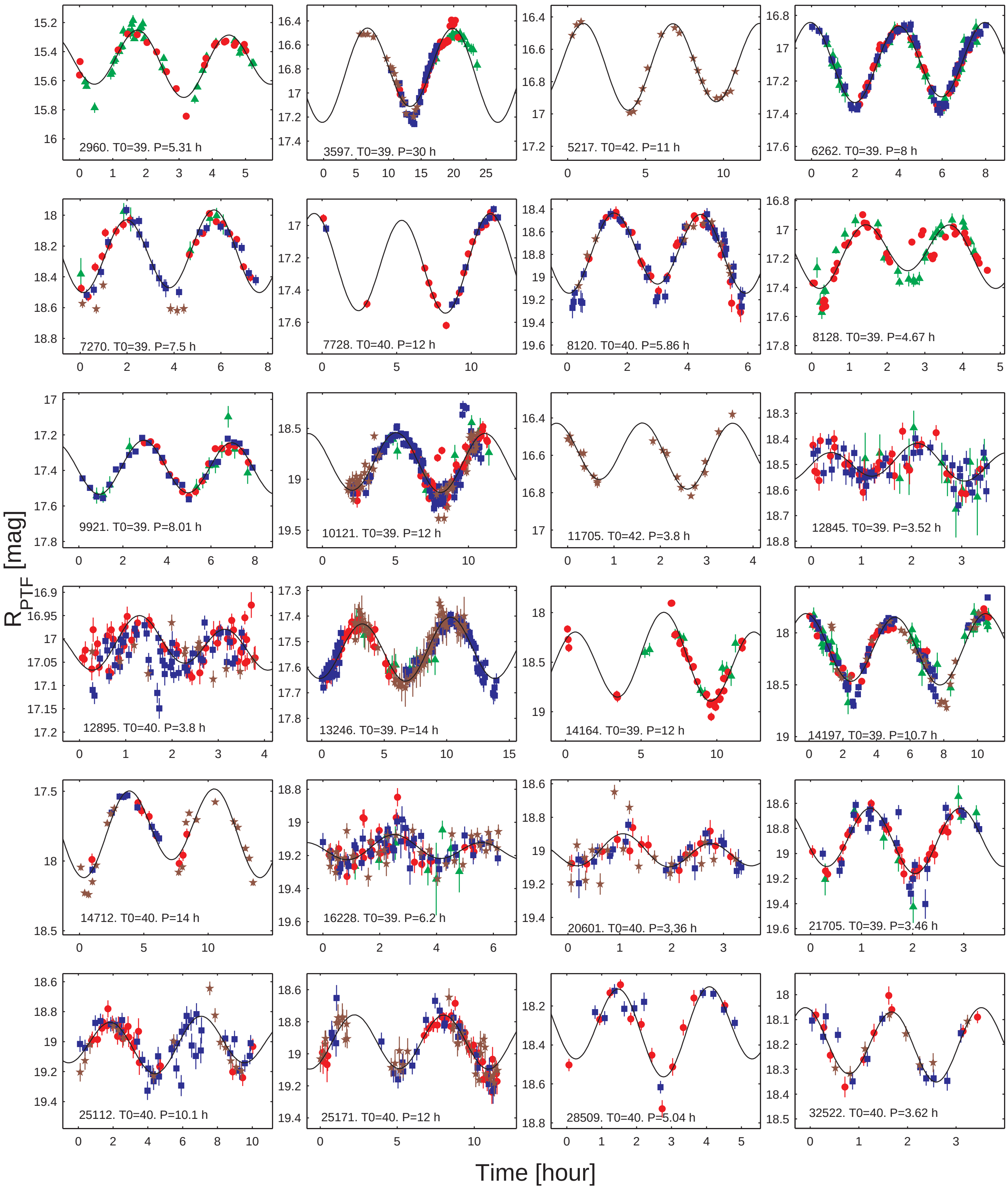

FIG. 6.— Set of 24 folded lightcurves. Reference epoch is $T_0 + 2455200$. Different markers indicate the observation date: 2010, Feb 12 - green triangles; 2010, Feb 13 - red circles; 2010, Feb 14 - blue squares; 2010, Feb 15 - brown pentagons. The designation of each asteroid, T_0 and the synodic rotation period P are given at the bottom of each plot.

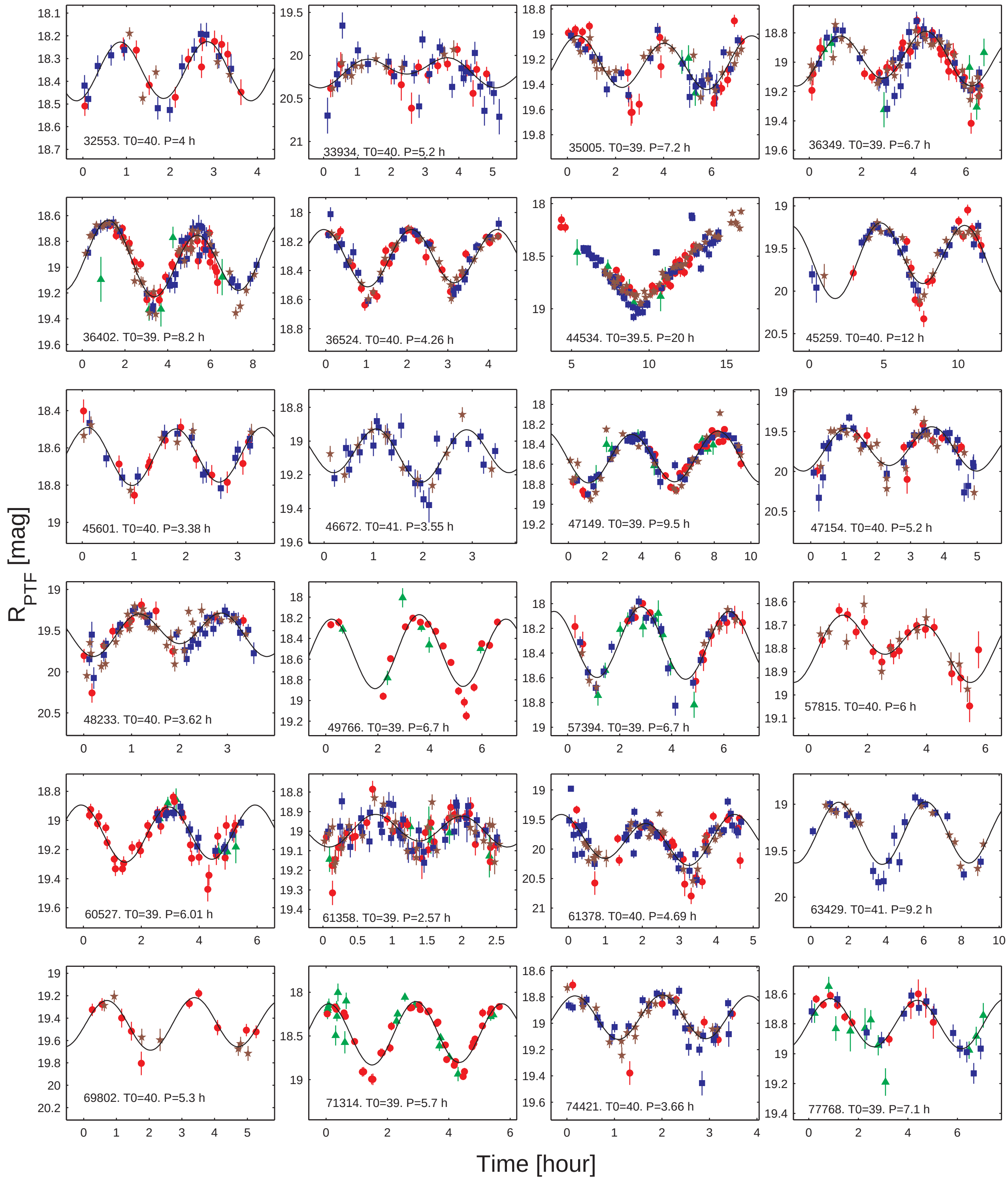

FIG. 7.— Same as Fig. 6 for 24 additional asteroids.

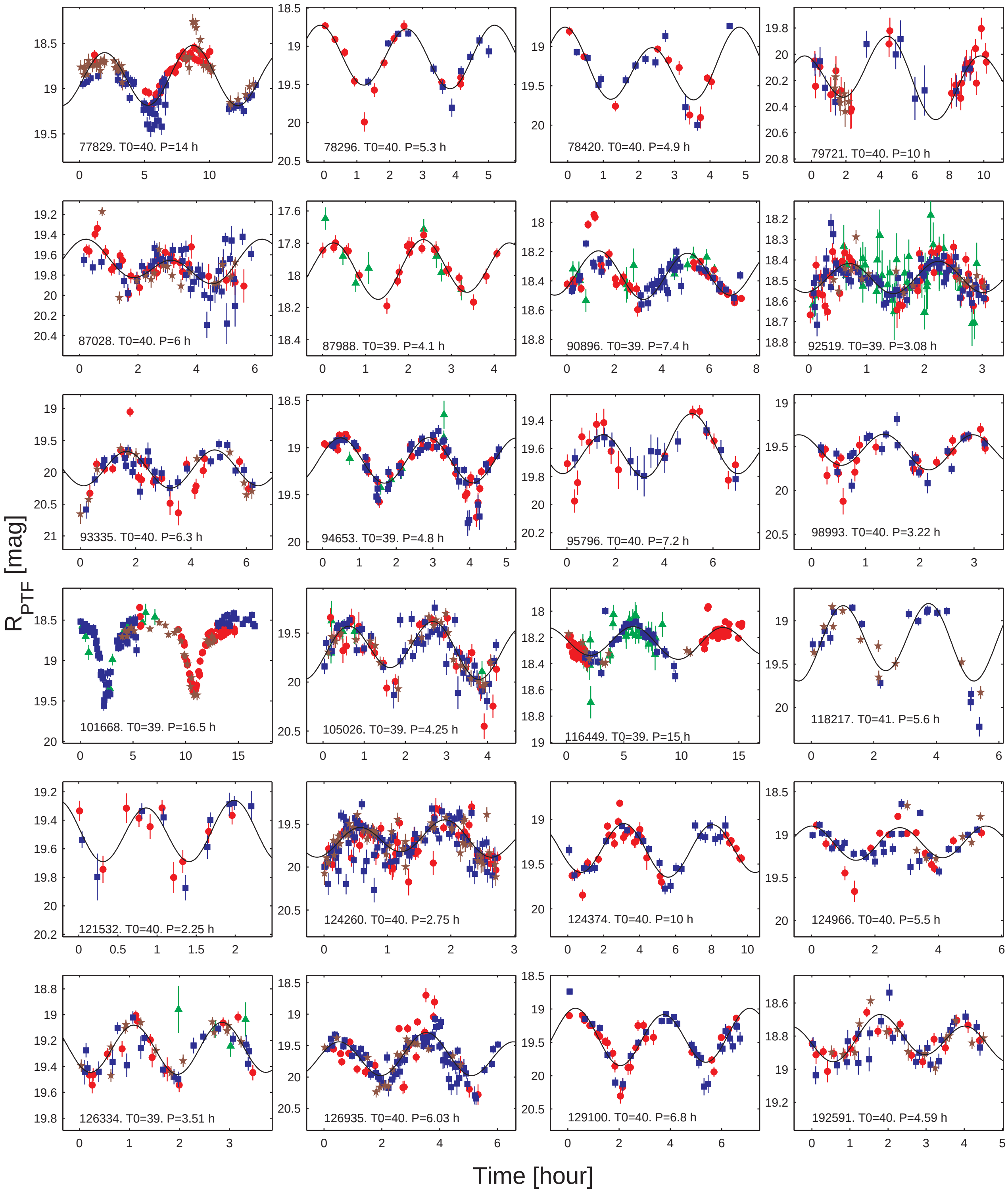

Fig. 8.— Same as Fig. 6-7 for 24 additional asteroids. The deep V-shaped minima and the inverted-U-shaped maxima of asteroid (101668) 1999 CR_{95} suggest a binary nature.

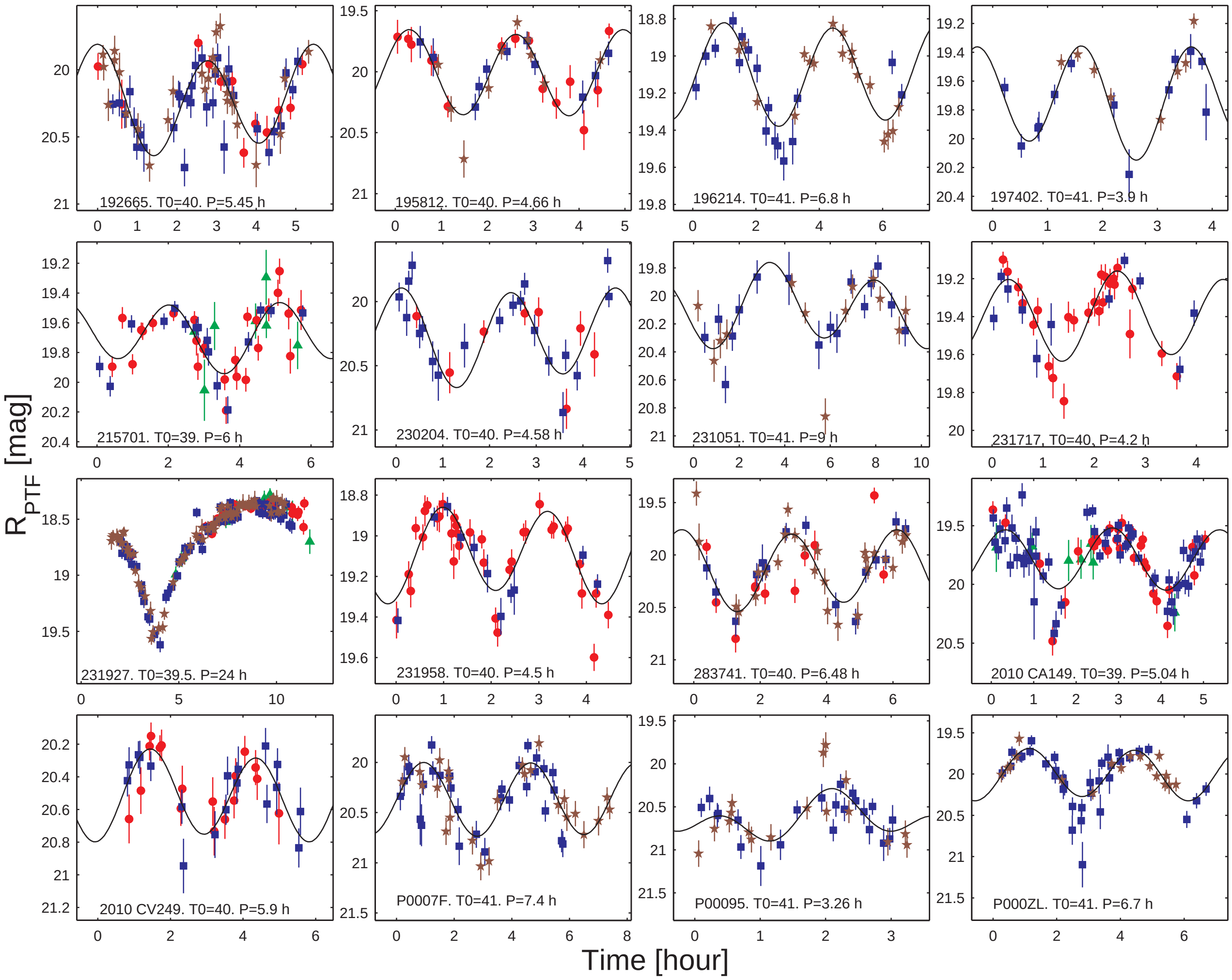

FIG. 9.— Same as Fig. 6-8 for 16 additional asteroids. The deep V-shaped minima and the inverted-U-shaped maxima of asteroid (231927) 2001 DU_{30} suggest a binary nature.

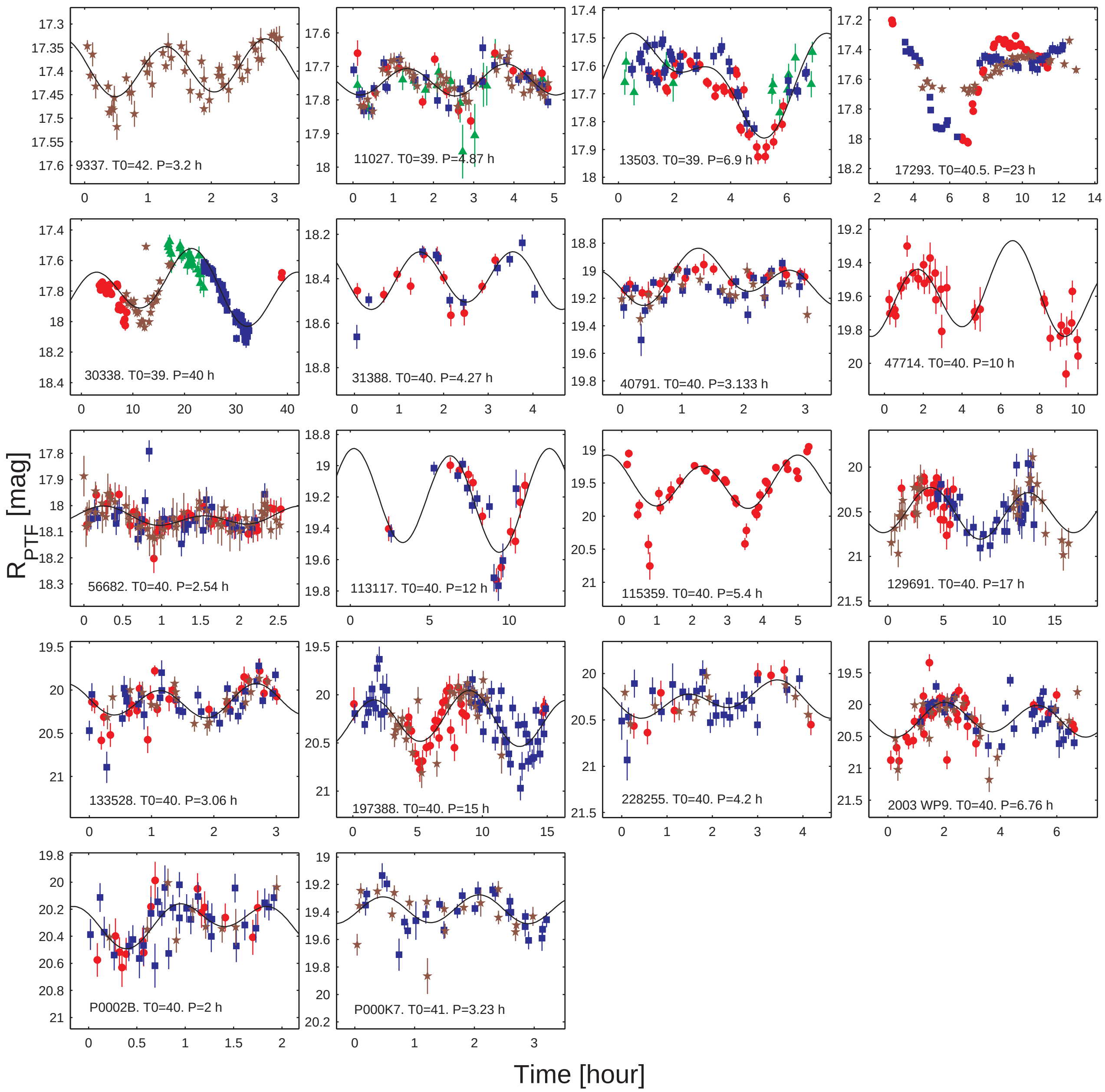

FIG. 10.— Set of 18 folded lightcurves with uncertain rotation periods (U=1). See Fig. 6 for symbols description. The deep V-shaped minima of asteroid (17293) 2743 P-L and the inconsistency of the peak's shape between different nights, suggest a binary nature.

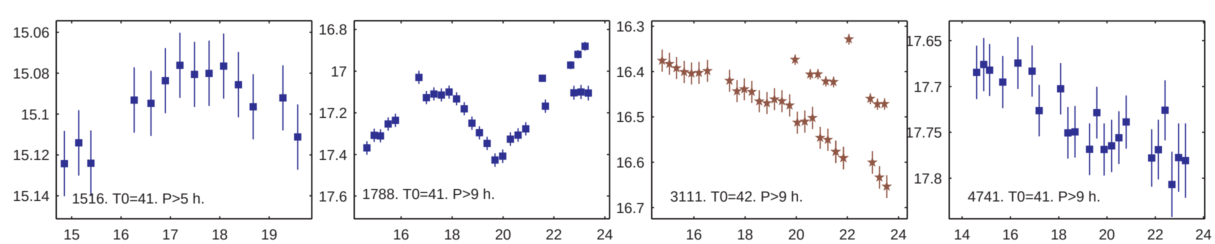

FIG. 11.— Set of 4 lightcurves with lower limits on the rotation periods. We only present data that show a continuous and convincing magnitude variability (the amplitude is larger than the photometric error) from a single night/CCD set that is the longest in time. See Fig. 6 for symbols description. This figure is published in its entirety in the electronic edition of *MNRAS*. A portion of the full figure is shown here for guidance regarding its form and content.

TABLE 6
All measurements of the detected asteroids

Designation	Field	CCD	JD	RA	Dec	R_{PTF}	AM	Background	$\langle FWHM \rangle$	r	Δ	α	a	e	i
			[day]	[deg]	[deg]	[mag]		[counts]	[arcsec]	[AU]	[AU]	[deg]	[AU]		[deg]
(625) Xenia	110001	01	2455239.7052872	127.88457	19.86213	14.4627±0.0244	1.15	1165.51	2.18	3.202	2.249	5.464	2.647	0.225	12.057
(625) Xenia	110002	07	2455239.7070572	127.88419	19.86229	14.5167±0.0352	1.14	1120.50	2.15	3.202	2.249	5.465	2.647	0.225	12.057
(625) Xenia	110001	01	2455239.7176472	127.88195	19.86330	14.4548±0.0245	1.12	1322.92	2.16	3.202	2.249	5.469	2.647	0.225	12.057
(625) Xenia	110002	07	2455239.7194372	127.88157	19.86346	14.5010±0.0352	1.11	1134.90	2.31	3.202	2.249	5.469	2.647	0.225	12.057
(625) Xenia	110001	01	2455239.7300672	127.87931	19.86446	14.4486±0.0249	1.09	2019.15	3.18	3.202	2.249	5.473	2.647	0.225	12.057

NOTE. — Columns: asteroids' designations, PTF's field and CCD, JD, RA, Dec, calibrated magnitude, air mass, image's background count and FWHM. The last six parameters are given only for objects with known orbital parameters: geocentric (r) and heliocentric (Δ) distances, phase angle (α), semi-major axis, eccentricity and inclination. This table is published in its entirety in the electronic edition of *MNRAS*. A portion of the full table is shown here for guidance regarding its form and content.

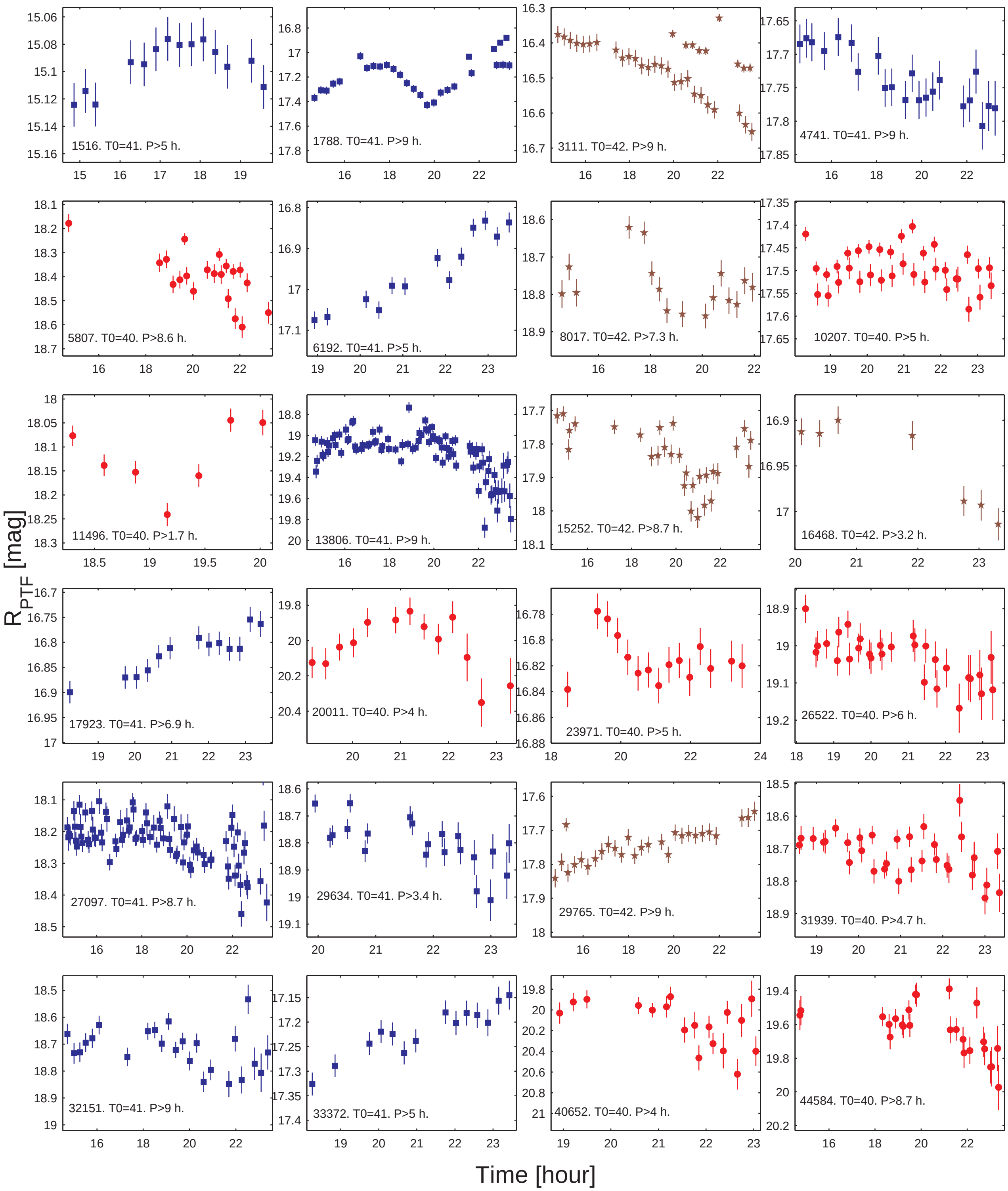

FIG. 11.— Set of 24 lightcurves with lower limits on the rotation periods. We only present data that show a continuous and convincing magnitude variability (the amplitude is larger than the photometric error) from a single night/CCD set that is the longest in time. Reference epoch is $T_0 + 2455200$. Different markers indicate the observation date: 2010, Feb 12 - green triangles; 2010, Feb 13 - red circles; 2010, Feb 14 - blue squares; 2010, Feb 15 - brown pentagons. The designation of each asteroid, T_0 and the synodic rotation period P are given at the bottom of each plot.

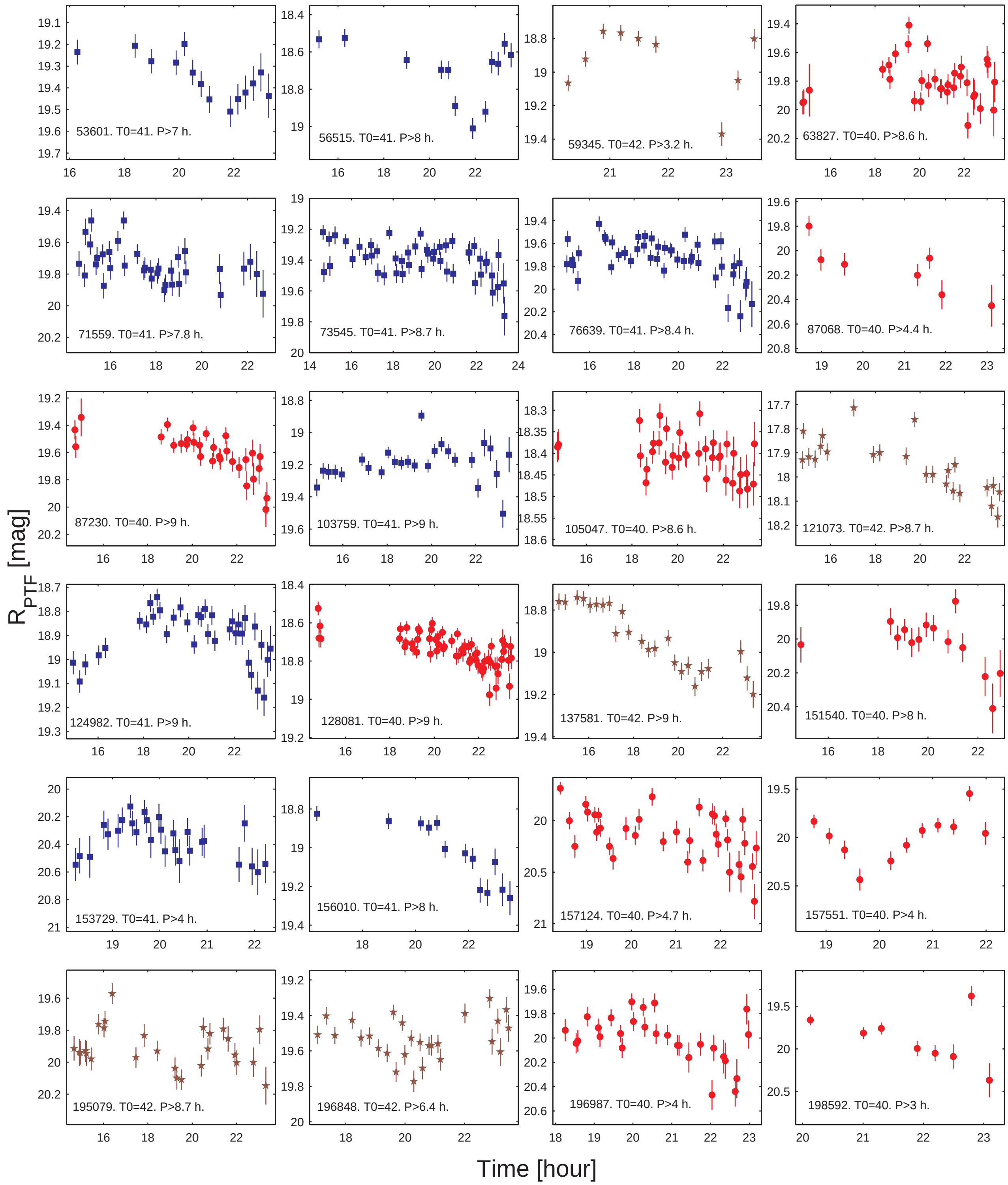

FIG. 12.— Same as Fig. 11 for 24 additional asteroids. See legend in the caption of Fig. 11.

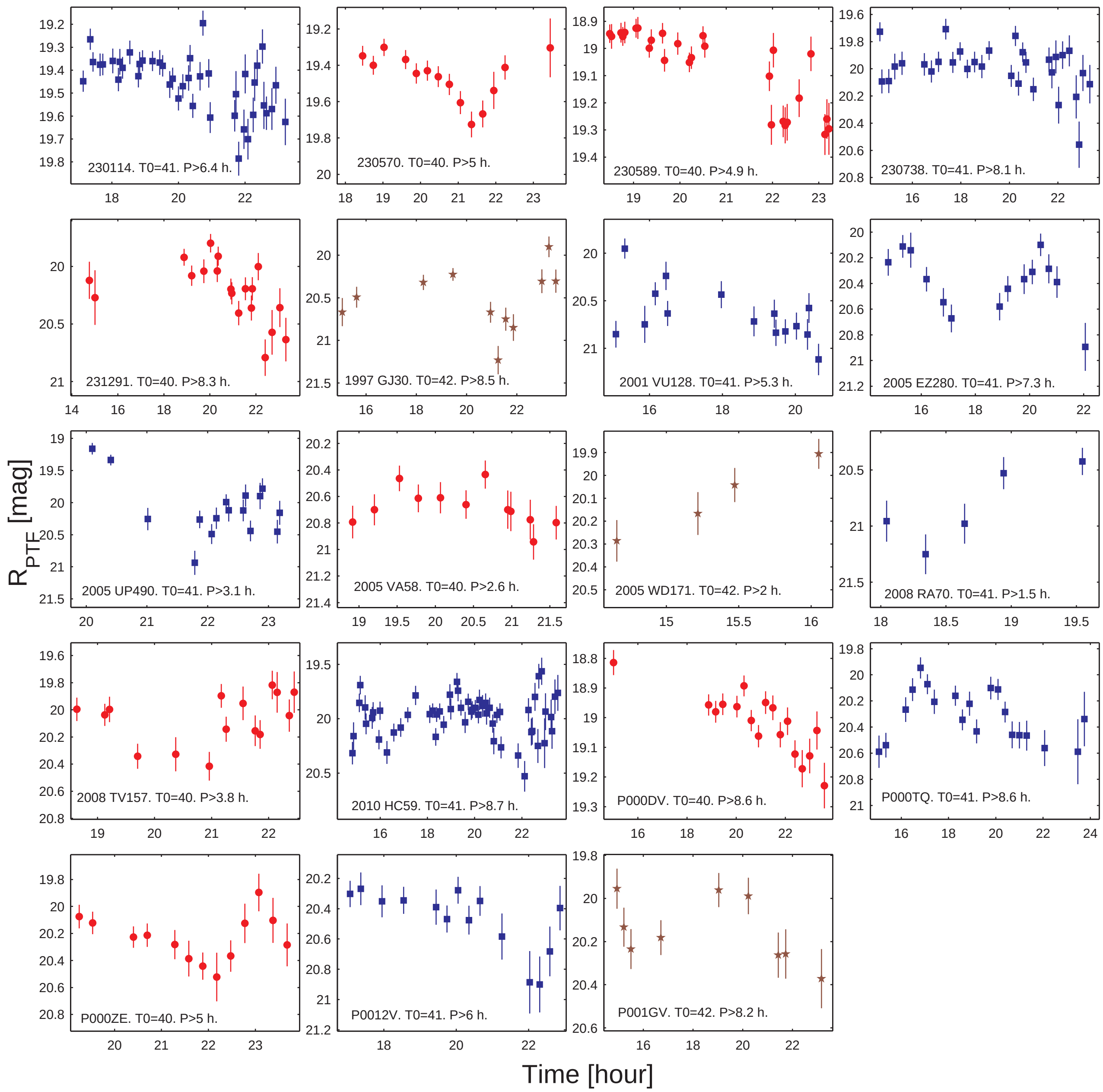

FIG. 13.— Same as Fig. 11-12 for 19 additional asteroids. See legend in the caption of Fig. 11.

TABLE 4
Lower limits on the synodic rotation periods of 67 asteroids

Designation	N_{nights}	N_{im}	r [AU]	Δ [AU]	α [deg]	Period [hour]	Amp [mag]	$\langle R_{PTF} \rangle$ [mag]	a [AU]
(1516) Henry	2	23	2.48	1.51	6.3	$\gtrsim 5$	$\gtrsim 0.03$	15.13 ± 0.02	2.62
(1788) Kiess	2	37	3.61	2.65	4.9	$\gtrsim 9$	$\gtrsim 0.8$	17.29 ± 0.03	3.11
(3111) Misuzu	1	38	2.29	1.33	7.2	$\gtrsim 9$	$\gtrsim 0.18$	16.47 ± 0.02	2.22
(4741) Leskov	3	46	3.68	2.74	5.2	$\gtrsim 9$	$\gtrsim 0.1$	17.85 ± 0.03	3.22
(5807) Mshatka	3	49	3.37	2.42	5.4	$\gtrsim 8.6$	$\gtrsim 0.3$	18.06 ± 0.04	3.05
(6192) 1990 KB1	2	25	2.82	1.86	5.8	$\gtrsim 5$	$\gtrsim 0.15$	16.85 ± 0.03	2.29
(8017) 1990 RM5	4	106	2.87	1.92	6.9	$\gtrsim 7.3$	$\gtrsim 0.29$	18.84 ± 0.05	2.36
(10207) Comeniana	3	97	2.58	1.63	7.5	$\gtrsim 5$	$\gtrsim 0.1$	17.51 ± 0.03	2.41
(11496) Grass	3	52	2.79	1.84	7	$\gtrsim 1.7$	$\gtrsim 0.15$	18.13 ± 0.03	2.61
(13806) Darmstrong	4	200	3.16	2.21	5.3	$\gtrsim 9$	$\gtrsim 0.4$	19.15 ± 0.06	2.94
(15252) 1990 OD1	4	148	2.57	1.62	7.3	$\gtrsim 8.7$	$\gtrsim 0.26$	17.78 ± 0.03	2.32
(16468) 1990 HW1	1	7	2.46	1.51	8.1	$\gtrsim 3.2$	$\gtrsim 0.1$	16.95 ± 0.02	2.56
(17923) 1999 GY16	3	29	2.26	1.3	7.9	$\gtrsim 6.9$	$\gtrsim 0$	17.04 ± 0.03	2.43
(20011) 1991 PD13	2	27	3.12	2.17	5.9	$\gtrsim 4$	$\gtrsim 0.63$	20.03 ± 0.1	2.6
(23971) 1998 YU9	3	45	2.41	1.44	6.8	$\gtrsim 5$	$\gtrsim 0.05$	16.8 ± 0.03	2.36
(26522) 2000 CZ83	4	137	3.25	2.3	5.7	$\gtrsim 6$	$\gtrsim 0.18$	18.85 ± 0.05	2.99
(27097) 1998 UM26	4	224	2.61	1.65	6.7	$\gtrsim 8.7$	$\gtrsim 0.13$	18.21 ± 0.04	2.26
(29634) 1998 VB3	3	99	3.23	2.28	5.9	$\gtrsim 3.4$	$\gtrsim 0.25$	18.78 ± 0.04	2.92
(29765) 1999 CG23	4	112	2.16	1.2	8.3	$\gtrsim 9$	$\gtrsim 0.16$	17.82 ± 0.03	2.38
(31939) 2000 GC101	4	133	2.71	1.76	7	$\gtrsim 4.7$	$\gtrsim 0.31$	18.79 ± 0.05	2.31
(32151) 2000 LX31	3	57	2.5	1.55	7.6	$\gtrsim 9$	$\gtrsim 0.45$	18.61 ± 0.04	2.37
(33372) 1999 BP23	3	50	2.13	1.17	8.8	$\gtrsim 5$	$\gtrsim 0.14$	17.25 ± 0.03	2.36
(40652) 1999 RP189	3	86	3.02	2.06	5.6	$\gtrsim 4$	$\gtrsim 0.55$	20.07 ± 0.1	2.63
(44584) 1999 JO21	4	98	2.63	1.68	6.9	$\gtrsim 8.7$	$\gtrsim 0.28$	19.59 ± 0.08	2.47
(53601) 2000 CK72	1	15	2.37	1.4	6.7	$\gtrsim 7$	$\gtrsim 0.62$	19.32 ± 0.07	2.24
(56515) 2000 HD20	2	20	2.29	1.32	6.6	$\gtrsim 8$	$\gtrsim 0.3$	18.66 ± 0.05	2.35
(59345) 1999 CK135	1	9	2.7	1.74	6.1	$\gtrsim 3.2$	$\gtrsim 0.46$	18.93 ± 0.05	2.43
(63827) 2001 RP71	1	32	2.52	1.57	7.7	$\gtrsim 8.6$	$\gtrsim 0.53$	19.8 ± 0.09	2.34
(71559) 2000 DU22	3	115	3.45	2.51	5.7	$\gtrsim 7.8$	$\gtrsim 0.71$	19.77 ± 0.08	2.98
(73545) 2003 OB31	3	111	3.08	2.14	6.5	$\gtrsim 8.7$	$\gtrsim 0.35$	19.32 ± 0.06	2.77
(76639) 2000 HP15	3	114	2.84	1.89	6.9	$\gtrsim 8.4$	$\gtrsim 0.4$	19.69 ± 0.08	3.06
(87068) 2000 KN58	3	38	2.88	1.92	6	$\gtrsim 4.4$	$\gtrsim 0.65$	20.4 ± 0.1	2.36
(87230) 2000 OZ42	3	106	2.72	1.77	7.1	$\gtrsim 9$	$\gtrsim 0.68$	19.84 ± 0.09	2.53
(103759) 2000 CG125	4	67	2.4	1.44	6.9	$\gtrsim 9$	$\gtrsim 0.36$	19.19 ± 0.06	2.24
(105047) 2000 KG52	4	140	2.61	1.65	7.2	$\gtrsim 8.6$	$\gtrsim 0.16$	18.45 ± 0.04	3.09
(121073) 1999 EL12	3	44	2.11	1.15	7.9	$\gtrsim 8.7$	$\gtrsim 0.36$	17.99 ± 0.04	2.42
(124982) 2001 TC130	3	83	2.08	1.12	8.7	$\gtrsim 9$	$\gtrsim 0.38$	18.88 ± 0.05	2.38
(128081) 2003 OO21	3	89	2.44	1.48	7	$\gtrsim 9$	$\gtrsim 0.24$	18.77 ± 0.05	2.66
(137581) 1999 VV137	3	64	2.08	1.12	9	$\gtrsim 9$	$\gtrsim 0.37$	18.9 ± 0.04	2.19
(151540) 2002 SR14	2	23	2.31	1.35	7.6	$\gtrsim 8$	$\gtrsim 0.54$	20.14 ± 0.1	2.12
(153729) 2001 UW122	3	70	2.69	1.73	6.3	$\gtrsim 4$	$\gtrsim 0.65$	20.3 ± 0.1	2.41
(156010) 2001 RQ75	2	27	2.37	1.4	6.6	$\gtrsim 8$	$\gtrsim 0.38$	19.03 ± 0.05	2.42
(157124) 2004 NJ13	4	88	2.61	1.65	6.8	$\gtrsim 4.7$	$\gtrsim 0.62$	20.1 ± 0.1	2.42
(157551) 2005 UZ66	1	13	2.32	1.36	7.3	$\gtrsim 4$	$\gtrsim 1.05$	20.05 ± 0.1	2.36
(195079) 2002 CL107	3	95	2.33	1.38	8.5	$\gtrsim 8.7$	$\gtrsim 0.44$	20.01 ± 0.09	2.58
(196848) 2003 SQ259	1	27	2.63	1.67	6.1	$\gtrsim 6.4$	$\gtrsim 0.3$	19.53 ± 0.06	3.05
(196987) 2003 UO81	2	65	3.17	2.22	5.7	$\gtrsim 4$	$\gtrsim 0.51$	20.02 ± 0.1	2.99
(198592) Antbernal	1	8	2.97	2.01	5.2	$\gtrsim 3$	$\gtrsim 0.84$	19.9 ± 0.1	2.82
(230114) 2001 BR71	3	143	2.56	1.6	7	$\gtrsim 6.4$	$\gtrsim 0.65$	19.47 ± 0.07	2.73
(230570) 2003 BQ64	1	15	1.97	1.01	9.7	$\gtrsim 5$	$\gtrsim 0.42$	19.45 ± 0.07	2.29
(230589) 2003 EM12	3	51	2.08	1.12	8.9	$\gtrsim 4.9$	$\gtrsim 0.57$	19.09 ± 0.06	2.37
(230738) 2003 WO10	2	59	2.95	2	5.8	$\gtrsim 8.1$	$\gtrsim 0.51$	19.96 ± 0.1	3
(231291) 2006 BZ102	3	44	2.75	1.8	6.8	$\gtrsim 8.3$	$\gtrsim 0.62$	20.2 ± 0.1	2.58
1997 GJ30	1	11	2.16	1.2	7.6	$\gtrsim 8.5$	$\gtrsim 1.13$	20.5 ± 0.1	2.22
2001 VU128	2	35	2.33	1.38	7.8	$\gtrsim 5.3$	$\gtrsim 0.64$	20.6 ± 0.2	2.32
2005 EZ280	2	34	2.73	1.77	6.1	$\gtrsim 7.3$	$\gtrsim 0.67$	20.5 ± 0.1	3.07
2005 UP490	2	64	2.15	1.19	8.2	$\gtrsim 3.1$	$\gtrsim 0.41$	20.3 ± 0.1	2.32
2005 VA58	1	17	2.47	1.52	7.8	$\gtrsim 2.6$	$\gtrsim 0.55$	20.6 ± 0.1	2.27
2005 WD171	3	73	2.13	1.17	9	$\gtrsim 2$	$\gtrsim 0.54$	19.95 ± 0.09	2.4
2008 RA70	3	23	2.41	1.45	6.8	$\gtrsim 1.5$	$\gtrsim 0.45$	20.8 ± 0.2	2.17
2008 TV157	3	28	3.01	2.05	5.7	$\gtrsim 3.8$	$\gtrsim 0.55$	20.1 ± 0.1	2.98
2010 HC59	2	93	2.35	1.39	7.5	$\gtrsim 8.7$	$\gtrsim 0.51$	20 ± 0.1	2.8
P000DV	1	17	...	...	...	$\gtrsim 8.6$	$\gtrsim 0.38$	19.02 ± 0.05	...
P000TQ	2	41	...	...	...	$\gtrsim 8.6$	$\gtrsim 0.57$	20.3 ± 0.1	...
P000ZE	2	44	...	...	...	$\gtrsim 5$	$\gtrsim 0.63$	20.2 ± 0.1	...
P0012V	1	15	...	...	...	$\gtrsim 6$	$\gtrsim 0.94$	20.4 ± 0.1	...
P001GV	1	9	...	...	...	$\gtrsim 8.2$	$\gtrsim 0.35$	20.15 ± 0.1	...

Note. — Columns: asteroids' designations, number of nights, number of images, geocentric (r) and heliocentric (Δ) distances, phase angle (α), limit on the rotation period, lightcurve amplitude, mean magnitude, semi-major axis.

TABLE 5
Lower limits on the amplitude of 451 asteroids

Designation	N_{nights}	N_{im}	r [AU]	Δ [AU]	α [deg]	Amp [mag]	$\langle R_{PTF} \rangle$ [mag]	a [AU]
(625) Xenia	3	57	3.2	2.25	5.8	$\gtrsim 0$	14.49 ± 0.02	2.65
(1079) Mimosa	2	14	2.8	1.84	5.77	$\gtrsim 0.1$	14.95 ± 0.04	2.87
(3679) Condruses	2	23	2.34	1.38	7.65	$\gtrsim 0.1$	15.13 ± 0.02	2.2
(5179) Takeshima	2	37	2.22	1.26	7.21	$\gtrsim 0.1$	17.29 ± 0.03	2.31
(6916) Lewispearce	2	57	3.2	2.25	5.34	$\gtrsim 0.3$	15.42 ± 0.02	2.84
(12992) 1981 EZ22	1	38	2.61	1.66	7.03	$\gtrsim 0.3$	16.47 ± 0.02	2.21
(13375) 1998 VH26	4	97	2.88	1.92	6.01	$\gtrsim 0.1$	16.78 ± 0.03	2.93
(13743) Rivkin	1	10	2.56	1.6	6.96	$\gtrsim 0.2$	17.2 ± 0.03	2.24
(14132) 1998 QB106	3	46	2.45	1.48	6.58	$\gtrsim 0.3$	17.85 ± 0.03	2.28
(15420) Aedouglass	2	31	3.35	2.4	5.71	$\gtrsim 0.4$	16.79 ± 0.04	2.65
(18797) 1999 JT64	1	20	3.08	2.13	5.75	$\gtrsim 0.3$	16.73 ± 0.01	2.59
(21358) Mijerbarany	3	49	2.81	1.86	7.24	$\gtrsim 0.3$	18.06 ± 0.04	2.75
(25825) 2000 DH88	2	25	3.33	2.37	4.81	$\gtrsim 0.1$	16.85 ± 0.03	3.02
(26904) 1995 YE25	3	155	2.74	1.78	6.56	$\gtrsim 0.6$	17.11 ± 0.03	2.29
(27379) 2000 EM58	3	89	3.48	2.53	4.6	$\gtrsim 0.5$	16.46 ± 0.02	3.09
(28612) 2000 FE2	4	56	3.16	2.2	5.16	$\gtrsim 0.3$	18.25 ± 0.04	3.07
(32551) 2001 QF22	2	27	2.62	1.65	5.93	$\gtrsim 0.5$	17.18 ± 0.02	2.37
(32632) 2001 RS75	4	106	2.67	1.7	5.63	$\gtrsim 0.3$	18.84 ± 0.05	2.4
(32964) 1996 PS3	3	79	2.47	1.51	7.83	$\gtrsim 0.3$	18.8 ± 0.05	2.42
(36422) 2000 OS67	2	74	2.82	1.87	6.79	$\gtrsim 0.8$	17.19 ± 0.03	2.41
(36874) 2000 SF151	1	52	2.53	1.57	7.15	$\gtrsim 0.1$	17.46 ± 0.02	2.58
(38676) 2000 PR15	3	55	2.59	1.63	5.95	$\gtrsim 0.7$	17.37 ± 0.02	2.56
(40627) 1999 RJ173	4	192	3.05	2.11	6.43	$\gtrsim 0.4$	18.87 ± 0.05	2.68
(43124) 1999 XJ53	3	97	2.96	2.01	5.8	$\gtrsim 0.3$	17.51 ± 0.03	2.78
(44002) 1997 ST1	4	106	3.43	2.48	5.66	$\gtrsim 1.1$	17.75 ± 0.03	3.01
(47700) 2000 CQ121	3	52	3.01	2.05	5.51	$\gtrsim 0.4$	18.13 ± 0.03	2.92
(47725) 2000 DW39	1	20	3.07	2.11	6.01	$\gtrsim 0.2$	16.65 ± 0.02	2.99
(50135) 2000 AU127	3	86	2.38	1.43	8.03	$\gtrsim 0.2$	18.51 ± 0.04	2.24
(50577) 2000 EU40	3	128	3.06	2.1	5.5	$\gtrsim 0.2$	17.02 ± 0.02	3.04
(50966) 2000 GZ85	4	82	2.86	1.91	6.62	$\gtrsim 0.2$	19.11 ± 0.06	3.02
(52820) 1998 RS2	4	222	2.57	1.61	6.04	$\gtrsim 0.3$	17.48 ± 0.03	2.21
(52974) 1998 TE34	3	122	2.57	1.62	7.45	$\gtrsim 0.3$	17.91 ± 0.03	2.25
(53690) 2000 DK83	3	92	2.83	1.88	6.57	$\gtrsim 0.3$	17.65 ± 0.03	2.96
(54936) 2001 OA106	4	170	2.9	1.94	5.43	$\gtrsim 0.5$	18.82 ± 0.05	2.34
(56127) 1999 CC34	4	200	2.51	1.56	7.7	$\gtrsim 0.4$	19.15 ± 0.06	2.4
(58053) 2003 AP5	2	27	2.43	1.48	7.42	$\gtrsim 0.7$	18.63 ± 0.05	2.3
(58257) 1993 RN9	2	49	2.54	1.58	7.03	$\gtrsim 0.3$	18.54 ± 0.04	2.44
(58311) 1994 PA22	4	161	2.19	1.23	7.89	$\gtrsim 0.3$	18.17 ± 0.04	2.33
(58452) 1996 JG3	3	36	2.54	1.6	7.92	$\gtrsim 0.6$	17.83 ± 0.03	2.38
(59197) 1999 BN3	4	148	2.04	1.07	7.72	$\gtrsim 0.2$	17.78 ± 0.03	2.38
(59319) 1999 CT91	1	11	2.43	1.47	6.57	$\gtrsim 0.1$	20.3 ± 0.1	2.39
(60902) 2000 JX27	4	123	3.57	2.61	4.49	$\gtrsim 0.2$	19.17 ± 0.06	3.23
(61146) 2000 NO10	1	7	2.96	2	5.32	$\gtrsim 1.2$	16.95 ± 0.02	2.45
(61330) 2000 OT58	3	115	2.94	1.98	5.45	$\gtrsim 0.6$	17.53 ± 0.02	2.45
(61936) 2000 RZ7	3	29	3.09	2.13	5.17	$\gtrsim 0.4$	17.04 ± 0.03	2.55
(63191) 2000 YP106	3	61	2.86	1.91	7.16	$\gtrsim 0.5$	19.32 ± 0.06	2.63
(65287) 2002 HL11	2	27	2.64	1.68	6.21	$\gtrsim 0.3$	20.03 ± 0.1	2.66
(67008) 1999 XD122	3	59	3.06	2.11	6.68	$\gtrsim 0.4$	19.02 ± 0.05	2.77
(67045) 1999 XZ191	3	57	2.95	2	6.21	$\gtrsim 0.3$	18.7 ± 0.04	2.84
(68356) 2001 NH12	3	65	2.3	1.34	7.64	$\gtrsim 0$	18.91 ± 0.06	2.2
(69300) 1992 EH7	3	45	2.59	1.62	6.2	$\gtrsim 0.2$	16.8 ± 0.03	2.75
(71678) 2000 ET172	3	76	2.89	1.94	6.75	$\gtrsim 0.4$	19.06 ± 0.06	2.95
(72186) 2000 YH118	3	97	2.73	1.77	5.91	$\gtrsim 0.1$	18.99 ± 0.06	2.74
(72380) 2001 CF10	1	12	3.02	2.08	6.78	$\gtrsim 0.6$	18.77 ± 0.04	2.74
(72607) 2001 FH17	4	137	2.81	1.86	6.87	$\gtrsim 0.4$	18.85 ± 0.05	2.87
(73331) 2002 JK106	4	173	3.21	2.26	5.69	$\gtrsim 0.7$	19.03 ± 0.06	2.77
(73941) 1997 SN11	4	224	2.92	1.97	5.83	$\gtrsim 0.4$	18.21 ± 0.04	3.08
(78201) 2002 NM49	3	31	3.03	2.09	6.6	$\gtrsim 0.3$	19.66 ± 0.08	2.94
(78402) 2002 QW8	2	23	3.48	2.52	4.56	$\gtrsim 0.5$	18.28 ± 0.03	3.07
(78586) 2002 SU12	2	35	3.13	2.17	5.43	$\gtrsim 0.3$	19.45 ± 0.08	3.25
(79618) 1998 RY61	3	99	2.64	1.67	5.8	$\gtrsim 0.7$	18.78 ± 0.04	2.23
(79734) 1998 SH136	4	112	2.69	1.74	7.13	$\gtrsim 0.6$	17.82 ± 0.03	2.24
(82213) 2001 HK49	4	145	2.55	1.6	7.84	$\gtrsim 0.5$	17.82 ± 0.03	2.19
(85400) 1996 TD10	2	22	2.71	1.76	7.43	$\gtrsim 0.5$	18.41 ± 0.04	2.57
(86780) 2000 GO92	4	133	2.58	1.62	7.42	$\gtrsim 0.7$	18.79 ± 0.05	2.29
(86837) 2000 GH160	3	57	2.49	1.54	8.06	$\gtrsim 0.5$	18.61 ± 0.04	2.29
(86847) 2000 GV174	3	30	2.34	1.39	8.17	$\gtrsim 0.4$	18.2 ± 0.03	2.28
(87042) 2000 KX6	2	34	2.54	1.59	7.66	$\gtrsim 0.7$	19.98 ± 0.09	2.34
(88357) 2001 OX99	3	30	2.76	1.79	5.84	$\gtrsim 2.3$	18.35 ± 0.05	2.28
(91346) 1999 JR37	3	25	2.18	1.22	7.49	$\gtrsim 0.2$	19.15 ± 0.1	2.45

Note. — Columns: asteroids' designations, number of nights, number of images, geocentric (r) and heliocentric (Δ) distances, phase angle (α), lower limit on the lightcurve amplitude, mean magnitude, semi-major axis.

TABLE 5
CONTINUED

Designation	N_{nights}	N_{im}	r [AU]	Δ [AU]	α [deg]	Amp [mag]	$\langle R_{PTF} \rangle$ [mag]	a [AU]
(91455) 1999 RV49	3	56	2.41	1.44	6.49	$\gtrsim 0.3$	18.71 ± 0.04	2.67
(94798) 2001 XL155	3	50	2.72	1.76	6.39	$\gtrsim 0.5$	17.25 ± 0.03	2.43
(96532) 1998 RH69	3	54	2.48	1.53	7.96	$\gtrsim 0.3$	20.2 ± 0.1	2.98
(97681) 2000 GA9	4	72	2.55	1.59	7.41	$\gtrsim 0.3$	19.27 ± 0.06	3
(97777) 2000 KG16	4	104	3.7	2.74	4.2	$\gtrsim 0.3$	19.01 ± 0.05	3.22
(99698) 2002 JY31	4	110	2.47	1.51	7.02	$\gtrsim 0.4$	18.93 ± 0.05	2.66
(99880) 2002 PT91	2	38	3.19	2.23	5.34	$\gtrsim 0.4$	19.9 ± 0.1	3.02
(100595) 1997 PA2	3	81	3.22	2.26	5.23	$\gtrsim 0.5$	18.32 ± 0.03	2.94
(101340) 1998 TN4	4	91	2.9	1.94	5.4	$\gtrsim 0.4$	18.05 ± 0.03	2.84
(101409) 1998 VQ6	2	38	2.24	1.27	6.93	$\gtrsim 0.1$	19.76 ± 0.09	2.32
(103576) 2000 CG1	1	14	2.1	1.14	8.67	$\gtrsim 0.1$	19.79 ± 0.08	2.24
(104187) 2000 EJ98	3	86	2.93	1.99	6.61	$\gtrsim 0.5$	20.07 ± 0.1	2.96
(104666) 2000 GF141	3	64	3.11	2.16	5.92	$\gtrsim 0.4$	19.09 ± 0.05	3.07
(108636) 2001 NS3	3	107	3.4	2.44	4.59	$\gtrsim 0.3$	19.45 ± 0.07	3.24
(108897) 2001 PW4	1	12	2.55	1.59	6.92	$\gtrsim 0.5$	20.2 ± 0.1	2.33
(109286) 2001 QR121	4	144	3.07	2.12	5.7	$\gtrsim 0.5$	18.61 ± 0.04	3.14
(111935) 2002 GB40	4	98	2.56	1.6	7.18	$\gtrsim 0.4$	19.59 ± 0.08	2.63
(112838) 2002 QZ17	3	56	3.34	2.38	5	$\gtrsim 0.7$	19.54 ± 0.07	3.13
(113325) 2002 RQ205	3	33	2.93	1.97	5.46	$\gtrsim 0.6$	18.63 ± 0.05	2.99
(113622) 2002 TE62	2	37	2.98	2.02	5.28	$\gtrsim 0.2$	19.08 ± 0.05	3.06
(114744) 2003 HU20	4	100	3.16	2.2	5.02	$\gtrsim 0.3$	18.55 ± 0.04	2.54
(115616) 2003 UH112	3	64	3.04	2.08	4.81	$\gtrsim 0.4$	19.71 ± 0.08	2.94
(115619) 2003 UD115	2	28	2.96	2.01	6.66	$\gtrsim 0.6$	19.25 ± 0.07	2.88
(116302) 2003 YH61	1	34	2.97	2.02	6.48	$\gtrsim 0.4$	19.64 ± 0.07	3.19
(117308) 2004 VQ22	1	14	2.69	1.73	5.93	$\gtrsim 0.4$	19.03 ± 0.05	2.66
(118304) 1998 UQ20	3	79	2.61	1.65	5.31	$\gtrsim 0.5$	19.52 ± 0.07	2.3
(120458) 1990 SN5	2	24	2.95	1.99	5.49	$\gtrsim 0.5$	18.5 ± 0.04	2.34
(120464) 1991 PV5	2	15	2.73	1.78	7.32	$\gtrsim 0.5$	18.91 ± 0.05	2.26
(120497) 1993 FF50	3	37	2.76	1.8	5.43	$\gtrsim 0.5$	19.36 ± 0.08	2.31
(120811) 1998 HT17	3	70	2.45	1.48	6.21	$\gtrsim 0.2$	18.44 ± 0.04	2.58
(120845) 1998 KU63	1	6	2.21	1.25	8.45	$\gtrsim 0.4$	19.46 ± 0.08	2.6
(121029) 1999 BL29	3	86	2.21	1.25	7.37	$\gtrsim 0.4$	19.48 ± 0.07	2.38
(122323) 2000 QZ17	1	15	2.66	1.7	5.83	$\gtrsim 0.3$	19.32 ± 0.07	2.53
(122337) 2000 QA35	3	73	2.76	1.8	6.48	$\gtrsim 0.5$	19.02 ± 0.05	2.48
(122680) 2000 RX105	1	13	2.87	1.91	6.02	$\gtrsim 0.4$	18.89 ± 0.05	2.48
(123140) 2000 TD18	4	66	2.52	1.56	6.71	$\gtrsim 0.4$	19.32 ± 0.06	2.57
(123181) 2000 UW2	2	20	2.74	1.79	6.62	$\gtrsim 0.4$	18.66 ± 0.05	2.59
(123377) 2000 WA45	3	125	2.64	1.7	7.78	$\gtrsim 0.5$	18.05 ± 0.05	2.62
(123529) 2000 XA13	4	52	2.95	2	6.42	$\gtrsim 0.2$	18.29 ± 0.06	2.65
(124549) 2001 RQ130	2	30	2.05	1.09	9.19	$\gtrsim 0.4$	18.79 ± 0.04	2.36
(124611) 2001 SC43	1	7	2.47	1.51	6.85	$\gtrsim 0.4$	18.5 ± 0.09	2.38
(124785) 2001 SX254	2	68	2.46	1.5	7.33	$\gtrsim 0.4$	18.72 ± 0.05	2.4
(124826) 2001 SH315	3	113	2.64	1.69	7.51	$\gtrsim 0.6$	19.33 ± 0.06	2.37
(126006) 2001 YS50	2	72	2.91	1.95	5.48	$\gtrsim 0.5$	19.93 ± 0.09	2.42
(126007) 2001 YM51	1	21	2.88	1.92	5.42	$\gtrsim 0.5$	19.2 ± 0.07	2.42
(126172) 2002 AZ8	2	24	2.63	1.68	7.55	$\gtrsim 0.3$	18.6 ± 0.05	2.53
(126837) 2002 ER64	1	9	2.44	1.48	6.58	$\gtrsim 0.1$	18.93 ± 0.05	2.58
(127374) 2002 KE	3	59	2.97	2.02	6.1	$\gtrsim 0.2$	19.08 ± 0.05	2.69
(127988) 2003 HJ46	1	18	2.14	1.17	7.52	$\gtrsim 0.3$	19.38 ± 0.05	2.4
(129515) 1995 UX17	2	47	2.62	1.68	7.5	$\gtrsim 0.4$	19.61 ± 0.06	2.64
(132096) 2002 CW194	1	18	2.58	1.63	7.31	$\gtrsim 0.6$	20.1 ± 0.08	2.54
(132944) 2002 TS46	4	113	3.83	2.87	3.85	$\gtrsim 0.7$	19.01 ± 0.05	3.14
(133257) 2003 RE20	3	103	2.7	1.74	6.86	$\gtrsim 0.3$	19.84 ± 0.09	2.86
(133268) 2003 SY3	2	20	2.82	1.87	6.93	$\gtrsim 0.4$	20.1 ± 0.1	2.87
(133422) 2003 SL190	2	22	3.04	2.09	5.95	$\gtrsim 0.7$	19.82 ± 0.08	2.9
(134194) 2005 CL70	2	34	3	2.04	5.72	$\gtrsim 0.4$	19.29 ± 0.06	2.92
(141376) 2002 AZ60	1	32	1.8	0.84	9.85	$\gtrsim 0.3$	19.8 ± 0.09	1.93
(143711) 2003 UR136	1	30	3.04	2.09	5.89	$\gtrsim 0.6$	18.69 ± 0.03	2.86
(147641) 2004 JS13	2	37	2.23	1.27	6.99	$\gtrsim 0.4$	19.73 ± 0.07	2.2
(149028) 2002 AU128	1	11	2.07	1.1	7.8	$\gtrsim 0.2$	19.28 ± 0.05	1.93
(149622) 2004 EP33	3	158	2.54	1.6	8.22	$\gtrsim 0.5$	19.14 ± 0.05	2.17
(152864) 1999 XT143	1	15	2.58	1.63	7.66	$\gtrsim 0.5$	18.93 ± 0.05	2.21
(152878) 2000 AT140	2	18	2.25	1.29	7.34	$\gtrsim 0.4$	19.47 ± 0.07	2.21
(153012) 2000 JG87	2	56	2.67	1.71	6.06	$\gtrsim 0.8$	18.45 ± 0.05	2.32
(153503) 2001 RB129	3	115	2.41	1.46	8.08	$\gtrsim 0.5$	19.77 ± 0.08	2.3
(154296) 2002 TG287	4	107	2.48	1.52	7.22	$\gtrsim 0.6$	19.97 ± 0.1	2.19
(155634) 2000 GJ2	2	42	2.68	1.72	6.43	$\gtrsim 0.5$	18.24 ± 0.04	2.33
(156136) 2001 TY38	2	32	2.61	1.66	7.72	$\gtrsim 0.3$	19.92 ± 0.09	2.38
(156168) 2001 TO144	4	107	2.53	1.58	7.79	$\gtrsim 0.5$	19.09 ± 0.06	2.31
(156919) 2003 FY51	1	15	2.23	1.27	7.82	$\gtrsim 0.3$	19.66 ± 0.08	2.37

NOTE. — Columns: asteroids' designations, number of nights, number of images, geocentric (r) and heliocentric (Δ) distances, phase angle (α), lower limit on the lightcurve amplitude, mean magnitude, semi-major axis.

TABLE 5
CONTINUED

Designation	N_{nights}	N_{im}	r [AU]	Δ [AU]	α [deg]	Amp [mag]	$\langle R_{PTF} \rangle$ [mag]	a [AU]
(157971) 2000 GN53	3	111	2.45	1.5	7.31	$\gtrsim 0.2$	19.32 ± 0.06	2.31
(158514) 2002 EZ116	3	80	2.77	1.82	6.9	$\gtrsim 0.3$	19.86 ± 0.08	2.62
(158861) 2004 PC8	3	58	2.5	1.55	7.95	$\gtrsim 0.6$	18.98 ± 0.05	2.35
(158888) 2004 PS71	3	114	2.81	1.86	7.44	$\gtrsim 0.9$	19.69 ± 0.08	2.39
(159850) 2003 YC35	3	36	3.19	2.23	5.04	$\gtrsim 0.6$	18.77 ± 0.07	3.05
(160974) 2002 CL38	3	125	2.64	1.69	7.36	$\gtrsim 0.5$	18.86 ± 0.06	2.55
(161076) 2002 LY40	4	105	3.4	2.44	4.51	$\gtrsim 0.6$	19.58 ± 0.08	2.8
(161959) 2007 HH48	2	23	2.83	1.88	7.08	$\gtrsim 0.6$	19.22 ± 0.07	2.44
(165668) 2001 NG12	2	23	3.52	2.56	4.44	$\gtrsim 0.5$	20.1 ± 0.1	3.09
(167174) 2003 SL260	2	22	2.73	1.78	6.77	$\gtrsim 0.5$	19.33 ± 0.07	2.63
(167572) 2004 BD61	3	48	3.3	2.35	5.76	$\gtrsim 0.6$	19.44 ± 0.08	3.25
(168107) 2006 EQ41	2	39	2.63	1.67	6.19	$\gtrsim 0.5$	19.94 ± 0.09	2.7
(168243) 2006 KB90	3	44	3.31	2.35	5.21	$\gtrsim 0.4$	20.2 ± 0.1	3.01
(169747) 2002 OY24	3	43	2.97	2.02	5.95	$\gtrsim 0.5$	19.8 ± 0.1	2.92
(170716) 2004 BF48	3	54	3.27	2.31	4.66	$\gtrsim 0.4$	19.55 ± 0.07	3.23
(189125) 2001 XW55	3	77	2.85	1.9	6.59	$\gtrsim 0.4$	20.1 ± 0.1	2.41
(189309) 2005 YJ213	1	11	2.96	2.01	6.32	$\gtrsim 0.4$	19.88 ± 0.1	2.41
(189704) 2001 TN110	3	87	2.71	1.75	6.82	$\gtrsim 0.8$	19.57 ± 0.07	2.37
(190288) 1994 PG12	3	19	2.71	1.76	6.75	$\gtrsim 0.6$	20.7 ± 0.2	2.3
(190645) 2000 XC18	3	93	2.59	1.63	7.05	$\gtrsim 0.5$	19.77 ± 0.08	2.64
(190790) 2001 RQ20	1	12	2.61	1.66	7.24	$\gtrsim 0.8$	19.79 ± 0.08	2.32
(191006) 2001 YE109	3	38	2.81	1.85	6.64	$\gtrsim 0.5$	20.4 ± 0.1	2.44
(191067) 2002 CJ149	3	106	2.51	1.55	7.51	$\gtrsim 0.4$	19.84 ± 0.09	2.54
(191069) 2002 CA151	2	32	2.25	1.3	8.3	$\gtrsim 0.4$	17.92 ± 0.05	2.55
(191557) 2003 WT63	1	12	3	2.05	6.49	$\gtrsim 0.7$	20.6 ± 0.1	3.09
(192123) 2006 DJ59	3	91	2.61	1.66	7.86	$\gtrsim 0.3$	18.36 ± 0.04	2.71
(192493) 1998 HG42	1	28	2.66	1.71	7.3	$\gtrsim 1.1$	18.24 ± 0.03	2.62
(192582) 1998 YF18	2	38	3.04	2.09	5.93	$\gtrsim 0.5$	17.71 ± 0.02	2.98
(192732) 1999 TF192	4	186	2.94	1.98	5.5	$\gtrsim 0.8$	18.48 ± 0.05	2.79
(193005) 2000 ER5	3	65	2.78	1.82	5.57	$\gtrsim 0.4$	20 ± 0.1	2.98
(193309) 2000 SP303	3	92	2.32	1.36	7.36	$\gtrsim 0.3$	19.17 ± 0.06	2.62
(196262) 2003 EK10	3	139	2.14	1.18	8.98	$\gtrsim 0.5$	20.3 ± 0.1	2.35
(196365) 2003 FX113	2	30	2.11	1.15	7.96	$\gtrsim 0.3$	19.62 ± 0.08	2.37
(196467) 2003 JX8	4	72	2.37	1.41	7.32	$\gtrsim 0.7$	18.71 ± 0.04	2.43
(196485) 2003 KG10	3	83	2.45	1.48	6.54	$\gtrsim 0.6$	19.15 ± 0.06	2.43
(196690) 2003 SD70	1	4	2.95	2	6.96	$\gtrsim 0.5$	20.4 ± 0.2	2.93
(196846) 2003 SR257	2	46	2.9	1.95	6.09	$\gtrsim 0.5$	19.6 ± 0.07	2.85
(197030) 2003 UM126	3	176	2.84	1.89	6.66	$\gtrsim 0.4$	18.97 ± 0.06	3.01
(197146) 2003 UM258	1	31	2.59	1.63	6	$\gtrsim 0.5$	19.81 ± 0.09	3.01
(197240) 2003 WD60	1	8	3.37	2.4	4.39	$\gtrsim 0.7$	20.5 ± 0.1	2.97
(197302) 2003 WY129	2	25	2.9	1.95	6.4	$\gtrsim 0.5$	19.9 ± 0.1	3.03
(197329) 2003 WL158	2	33	3.01	2.07	6.72	$\gtrsim 0.5$	18.39 ± 0.03	2.95
(198296) 2004 TK309	4	178	2.73	1.78	6.46	$\gtrsim 0.4$	18.79 ± 0.05	2.58
(199085) 2005 XO104	4	100	3.12	2.16	4.89	$\gtrsim 0.4$	18.2 ± 0.04	2.58
(199342) 2006 BW157	4	67	2.49	1.52	6.25	$\gtrsim 0.6$	19.19 ± 0.06	2.63
(199550) 2006 EE15	1	17	2.96	2.01	6.75	$\gtrsim 0.5$	20.5 ± 0.1	2.77
(199769) 2006 KA22	3	61	3.19	2.23	5.52	$\gtrsim 0.5$	19.92 ± 0.09	3.08
(199876) 2007 EE198	4	109	2.25	1.29	7.23	$\gtrsim 0.6$	19.68 ± 0.08	2.29
(200320) 2000 FF69	4	140	2.85	1.9	7.28	$\gtrsim 0.5$	18.45 ± 0.04	3.06
(200703) 2001 UN94	1	5	2.51	1.54	6.2	$\gtrsim 0.4$	20.3 ± 0.1	2.4
(202535) 2006 DX43	3	116	2.69	1.73	6.1	$\gtrsim 0.5$	20.2 ± 0.1	2.57
(202829) 2008 SD160	4	108	2.94	2	6.93	$\gtrsim 0.5$	19.2 ± 0.06	2.66
(204923) 2008 SZ260	3	74	3.05	2.1	5.79	$\gtrsim 0.8$	19.56 ± 0.07	2.99
(212354) 2006 BQ101	3	20	2.96	2.01	6.84	$\gtrsim 0.8$	20.2 ± 0.1	2.52
(216033) 2006 AW67	2	24	2.7	1.75	7.37	$\gtrsim 0.5$	19.3 ± 0.07	2.42
(225872) 2001 XG260	1	28	2.11	1.16	9.48	$\gtrsim 0.6$	19.42 ± 0.05	2.43
(228092) 2008 SY6	2	27	2.91	1.95	5.77	$\gtrsim 0.7$	18.53 ± 0.08	2.71
(228510) 2001 TU91	1	7	2.46	1.5	7.79	$\gtrsim 1$	20.5 ± 0.1	2.4
(229443) 2005 UA51	1	36	2.36	1.41	8.43	$\gtrsim 0.7$	19.6 ± 0.08	2.34
(229524) 2005 XG11	1	10	2.05	1.08	7.66	$\gtrsim 0.2$	20.22 ± 0.1	2.39
(230106) 2001 AZ8	3	73	2.54	1.58	7.55	$\gtrsim 0.3$	20.2 ± 0.1	2.7
(230154) 2001 QV104	4	66	2.54	1.59	6.71	$\gtrsim 0.8$	19.31 ± 0.07	2.41
(230256) 2001 VM104	4	124	2.61	1.65	6.9	$\gtrsim 0.6$	18.24 ± 0.04	2.42
(230348) 2002 CM277	3	31	2.37	1.41	7.4	$\gtrsim 0.6$	19.69 ± 0.09	2.54
(230357) 2002 EJ32	2	28	2.63	1.68	6.81	$\gtrsim 0.5$	19.27 ± 0.06	2.57
(230511) 2002 VD38	2	18	2.32	1.35	6.4	$\gtrsim 0.4$	19.8 ± 0.1	2.19
(230597) 2003 ES45	2	11	2.06	1.1	8.88	$\gtrsim 0.5$	20.6 ± 0.1	2.36
(230605) 2003 FY38	2	18	2.19	1.24	9.26	$\gtrsim 0.6$	20.6 ± 0.1	2.38
(230639) 2003 QJ55	2	36	2.91	1.95	5.9	$\gtrsim 0.4$	20 ± 0.1	2.76
(230784) 2003 YZ150	3	30	2.75	1.79	5.76	$\gtrsim 0.4$	19.5 ± 0.1	3.26

NOTE. — Columns: asteroids' designations, number of nights, number of images, geocentric (r) and heliocentric (Δ) distances, phase angle (α), lower limit on the lightcurve amplitude, mean magnitude, semi-major axis.

TABLE 5
CONTINUED

Designation	N_{nights}	N_{im}	r [AU]	Δ [AU]	α [deg]	Amp [mag]	$\langle R_{PTF} \rangle$ [mag]	a [AU]
(230887) 2004 RW345	3	24	2.4	1.45	8.55	$\gtrsim 0.3$	18.37 ± 0.03	2.69
(230911) 2004 TR201	2	23	2.45	1.49	7.84	$\gtrsim 0.6$	19.46 ± 0.08	2.68
(231151) 2005 UR41	3	44	2.27	1.32	8.75	$\gtrsim 0.5$	17.99 ± 0.04	2.34
(231297) 2006 BT141	2	20	2.82	1.87	6.37	$\gtrsim 0.4$	19.48 ± 0.08	2.66
(231463) 2007 PO	2	23	3.01	2.06	5.8	$\gtrsim 0.3$	20.4 ± 0.1	3.14
(231532) 2008 SK126	1	12	2.72	1.76	5.83	$\gtrsim 0.6$	20.6 ± 0.1	2.94
(231555) 2008 TT2	3	30	3.02	2.06	5.51	$\gtrsim 0.8$	20.7 ± 0.1	2.93
(237344) 2010 AY23	3	46	2.03	1.07	9.48	$\gtrsim 0.8$	19.52 ± 0.08	2.23
(264158) 2010 AJ22	3	77	2.65	1.7	7.5	$\gtrsim 0.6$	19.54 ± 0.07	3.11
(269601) 2010 CX1	2	31	2.7	1.74	6.22	$\gtrsim 0.4$	19.97 ± 0.09	2.71
(279674) 2011 FU29	3	72	3.35	2.41	5.86	$\gtrsim 0.6$	19.5 ± 0.07	3.2
1994 TE11	3	190	2.21	1.26	8.38	$\gtrsim 0.4$	19.73 ± 0.08	2.36
1995 UK16	2	51	2.38	1.43	8.57	$\gtrsim 0.5$	19.33 ± 0.06	2.7
1999 RM169	3	55	3.16	2.22	6	$\gtrsim 0.5$	19.38 ± 0.07	2.69
2001 FU95	3	68	2.34	1.38	7.34	$\gtrsim 0.4$	19.87 ± 0.08	2.79
2001 SE60	2	21	2.55	1.59	6.52	$\gtrsim 0.3$	19.45 ± 0.07	2.29
2001 SZ265	3	64	2.49	1.53	6.59	$\gtrsim 0.3$	19.68 ± 0.07	2.41
2001 TE154	3	51	2.73	1.77	6.35	$\gtrsim 0.5$	19.11 ± 0.05	2.31
2001 UP145	3	83	2.38	1.41	6.61	$\gtrsim 0.6$	18.88 ± 0.05	2.42
2001 WS67	2	12	2.12	1.17	9.52	$\gtrsim 3.4$	20.2 ± 0.1	2.43
2001 XQ206	2	48	2.56	1.6	7.02	$\gtrsim 0.8$	20.3 ± 0.1	2.44
2002 AZ31	3	21	2.09	1.14	9.68	$\gtrsim 0.4$	20.4 ± 0.1	2.53
2002 CL11	4	53	2.31	1.34	6.62	$\gtrsim 0.9$	19.26 ± 0.06	2.53
2002 CY43	1	18	2.01	1.05	9.83	$\gtrsim 0.5$	19.3 ± 0.05	1.92
2002 LL1	3	116	2.9	1.94	5.47	$\gtrsim 0.5$	19.7 ± 0.08	2.74
2002 NO68	3	128	3.02	2.06	5.34	$\gtrsim 0.3$	19.34 ± 0.06	2.95
2002 QS99	2	19	3.12	2.17	6.37	$\gtrsim 0.4$	19.05 ± 0.06	2.97
2002 RQ20	3	89	2.2	1.24	7.73	$\gtrsim 0.5$	18.77 ± 0.05	2.17
2002 TK324	2	57	2.89	1.93	5.89	$\gtrsim 0.7$	19.51 ± 0.07	3.16
2003 BV49	1	9	2.05	1.09	8.5	$\gtrsim 0.3$	20.3 ± 0.1	2.3
2003 BT77	3	86	2.06	1.1	8.04	$\gtrsim 0.2$	20.4 ± 0.1	2.31
2003 FF131	1	17	2.13	1.17	8.6	$\gtrsim 0.8$	20.17 ± 0.09	2.36
2003 HM58	1	6	2.22	1.26	7.31	$\gtrsim 0.3$	20.6 ± 0.1	2.46
2003 SK333	1	16	3.19	2.23	5.56	$\gtrsim 0.3$	19.79 ± 0.07	2.81
2003 UK171	4	55	2.95	1.98	5.31	$\gtrsim 0.5$	19.65 ± 0.08	3.01
2003 UH357	2	26	2.88	1.93	5.8	$\gtrsim 0.3$	20 ± 0.1	2.99
2004 PC52	3	79	2.82	1.88	7.19	$\gtrsim 0.3$	20.1 ± 0.1	2.35
2004 RD143	3	78	2.72	1.76	6.33	$\gtrsim 0$	20.3 ± 0.1	2.57
2004 VO27	3	64	2.6	1.64	6.69	$\gtrsim 0.4$	18.9 ± 0.04	2.65
2004 VY90	1	36	2.74	1.78	5.78	$\gtrsim 0.7$	18.46 ± 0.03	2.66
2005 CY14	3	28	2.95	1.99	5.03	$\gtrsim 0.5$	20.4 ± 0.1	2.95
2005 EP5	3	65	2.7	1.74	6.05	$\gtrsim 0.5$	19.69 ± 0.08	3.09
2005 EA43	2	20	3.24	2.28	4.85	$\gtrsim 0.5$	18.66 ± 0.05	3.1
2005 EC99	1	6	3.04	2.08	5.42	$\gtrsim 0.7$	20.6 ± 0.2	3.06
2005 EK182	2	23	2.99	2.05	6.48	$\gtrsim 0.4$	20.14 ± 0.1	3.15
2005 FR14	3	24	3.07	2.11	5.17	$\gtrsim 0.7$	20.4 ± 0.1	3.17
2005 GJ128	2	19	2.89	1.94	6.62	$\gtrsim 0.4$	19.59 ± 0.09	3.16
2005 SP210	2	23	2.08	1.12	9.28	$\gtrsim 0.4$	20.4 ± 0.1	2.28
2005 SL289	2	38	2.09	1.12	7.63	$\gtrsim 0.7$	20.1 ± 0.1	2.31
2005 UK163	3	70	2.2	1.25	8.78	$\gtrsim 0.7$	20.3 ± 0.1	2.38
2005 UT292	2	41	2.06	1.1	9.48	$\gtrsim 0.6$	20.6 ± 0.1	2.36
2005 VC112	1	7	2.15	1.19	8.65	$\gtrsim 0.7$	20.9 ± 0.2	2.4
2005 WU86	2	27	2	1.03	7.75	$\gtrsim 1.1$	19.03 ± 0.05	2.4
2005 WX139	1	14	2.27	1.32	8.34	$\gtrsim 0.8$	19.51 ± 0.07	2.34
2005 WL197	2	35	2.07	1.11	8.27	$\gtrsim 0.6$	19.98 ± 0.09	2.39
2006 AO4	3	127	2.65	1.68	5.94	$\gtrsim 0.5$	19.33 ± 0.06	2.63
2006 AC90	4	88	2.31	1.34	6.71	$\gtrsim 0.6$	20.1 ± 0.1	2.64
2006 AZ94	1	13	2.34	1.39	8.25	$\gtrsim 1.1$	20.05 ± 0.1	2.46
2006 BE29	1	4	2.88	1.93	6.87	$\gtrsim 0.4$	20.7 ± 0.2	2.61
2006 BW41	1	6	2.32	1.36	8.39	$\gtrsim 0.5$	20.3 ± 0.1	2.62
2006 BB89	3	64	2.84	1.9	7.35	$\gtrsim 0.4$	20.3 ± 0.1	2.56
2006 BO135	1	3	2.8	1.84	5.95	$\gtrsim 0.3$	20.1 ± 0.1	2.56
2006 BV135	2	20	2.11	1.16	8.91	$\gtrsim 0.5$	19.69 ± 0.09	2.58
2006 DS23	3	79	2.39	1.43	7.49	$\gtrsim 0.5$	20.2 ± 0.1	2.62
2006 DA93	3	45	2.81	1.86	6.35	$\gtrsim 0.5$	20.5 ± 0.1	2.77
2006 DJ212	1	10	2.63	1.67	6.51	$\gtrsim 0.6$	20.9 ± 0.1	2.71
2006 DE217	3	43	2.68	1.72	5.99	$\gtrsim 0.4$	20.4 ± 0.1	2.67
2006 EP23	1	7	2.24	1.28	8.91	$\gtrsim 0.4$	20.5 ± 0.1	2.6
2006 GL30	2	19	2.93	1.96	5.29	$\gtrsim 0.3$	20.4 ± 0.1	2.87
2006 JL29	2	15	2.86	1.91	6.84	$\gtrsim 0.6$	20.2 ± 0.1	2.93

NOTE. — Columns: asteroids' designations, number of nights, number of images, geocentric (r) and heliocentric (Δ) distances, phase angle (α), lower limit on the lightcurve amplitude, mean magnitude, semi-major axis.

TABLE 5
CONTINUED

Designation	N_{nights}	N_{im}	r [AU]	Δ [AU]	α [deg]	Amp [mag]	$\langle R_{PTF}\rangle$ [mag]	a [AU]
2006 JM42	2	22	3.41	2.47	5.62	$\gtrsim 0.4$	20.5 ± 0.1	3.05
2006 KP31	3	37	2.75	1.8	7.19	$\gtrsim 0.4$	20.4 ± 0.1	2.94
2007 EE153	3	63	2.01	1.05	9.72	$\gtrsim 0.7$	19.75 ± 0.07	2.18
2007 EA198	1	8	2.4	1.44	7.74	$\gtrsim 0.3$	20.7 ± 0.2	2.27
2007 HE51	3	22	2.33	1.38	8.39	$\gtrsim 0.5$	20.2 ± 0.1	2.39
2007 JY18	2	25	2.21	1.26	8.62	$\gtrsim 0.5$	20.6 ± 0.1	2.36
2007 JY22	1	16	2.95	2	6.53	$\gtrsim 0.7$	20.4 ± 0.1	2.59
2007 JM24	2	51	2.69	1.74	7.17	$\gtrsim 0.4$	19.88 ± 0.1	2.55
2007 LF5	1	6	3.06	2.11	6.11	$\gtrsim 0.6$	20.9 ± 0.1	2.67
2007 QH	1	5	3.6	2.64	4.13	$\gtrsim 0.7$	20.4 ± 0.1	3.1
2008 ST110	1	14	2.95	2	6.37	$\gtrsim 0.4$	20.2 ± 0.1	3.23
2008 SY143	3	34	2.81	1.87	6.95	$\gtrsim 0.6$	19.5 ± 0.07	2.98
2008 SE198	3	36	2.98	2.02	5.46	$\gtrsim 0.4$	20.3 ± 0.1	2.97
2008 SR251	4	91	2.7	1.74	6.4	$\gtrsim 0.6$	19.59 ± 0.08	2.74
2008 SJ258	3	30	2.9	1.93	5.31	$\gtrsim 0.7$	20 ± 0.1	3.01
2008 SV282	3	82	2.83	1.86	5.35	$\gtrsim 0.5$	20.1 ± 0.1	2.74
2008 SN287	3	59	2.86	1.9	5.84	$\gtrsim 0.6$	18.83 ± 0.04	2.97
2008 SF304	3	73	2.53	1.58	7.98	$\gtrsim 0.3$	20.2 ± 0.1	2.61
2008 TA10	1	7	2.56	1.59	5.95	$\gtrsim 0.4$	20.2 ± 0.1	2.78
2008 TL51	3	92	2.77	1.82	6.93	$\gtrsim 1$	20.04 ± 0.1	3.15
2008 TM53	2	15	2.83	1.86	5.23	$\gtrsim 0.3$	19.48 ± 0.07	3.14
2008 TE67	3	95	2.77	1.81	6.33	$\gtrsim 0.3$	20.01 ± 0.09	2.78
2008 UU50	3	36	3.04	2.09	5.74	$\gtrsim 0.6$	19.99 ± 0.1	3.08
2008 UB242	2	36	3.02	2.07	5.98	$\gtrsim 0.5$	19.16 ± 0.06	2.84
2008 UQ242	3	47	3.21	2.25	5.22	$\gtrsim 0.6$	19.65 ± 0.08	3.17
2008 UZ286	1	4	3.06	2.11	5.66	$\gtrsim 0.3$	19.42 ± 0.07	3.42
2008 UL294	3	21	3.11	2.16	6.07	$\gtrsim 0.9$	19.54 ± 0.09	2.97
2008 UR302	1	9	3.87	2.93	5.26	$\gtrsim 1.3$	20.4 ± 0.1	3.93
2009 YP25	1	14	2.49	1.53	7.67	$\gtrsim 0.6$	20.5 ± 0.1	2.56
2010 AV22	3	96	2.5	1.54	7.18	$\gtrsim 0.5$	20.5 ± 0.1	2.98
2010 AR23	1	27	2.19	1.23	8.46	$\gtrsim 0.3$	19.53 ± 0.06	2.75
2010 AB34	2	65	2.9	1.96	6.73	$\gtrsim 0.7$	20.02 ± 0.1	3.14
2010 AH44	3	45	2.69	1.74	7.13	$\gtrsim 0.5$	20 ± 0.1	3.19
2010 AA76	2	39	3.32	2.36	4.83	$\gtrsim 0.5$	20.03 ± 0.08	3.16
2010 CW149	1	7	...	...	...	$\gtrsim 0.6$	20.7 ± 0.1	...
2010 FJ5	2	23	1.89	0.92	9.89	$\gtrsim 0.5$	20.3 ± 0.1	2.34
2010 HS27	2	11	2.65	1.71	7.64	$\gtrsim 0.6$	20.9 ± 0.2	3.02
P00011	3	108	...	...	...	$\gtrsim 0.9$	20.2 ± 0.1	...
P0001P	2	22	...	...	...	$\gtrsim 0.5$	19.71 ± 0.08	...
P0002H	3	26	...	...	...	$\gtrsim 0.5$	20.9 ± 0.2	...
P0002R	1	8	...	...	...	$\gtrsim 0.3$	19.9 ± 0.1	...
P00030	1	12	...	...	...	$\gtrsim 0.7$	20.7 ± 0.2	...
P00033	2	47	...	...	...	$\gtrsim 0.6$	20.4 ± 0.1	...
P0003C	3	33	...	...	...	$\gtrsim 0.5$	20.7 ± 0.1	...
P0003H	2	30	...	...	...	$\gtrsim 0.5$	20.1 ± 0.1	...
P0004A	2	17	...	...	...	$\gtrsim 0.8$	20.3 ± 0.1	...
P0004E	1	10	...	...	...	$\gtrsim 0.7$	20.5 ± 0.1	...
P0004U	2	57	...	...	...	$\gtrsim 0.5$	20.04 ± 0.09	...
P0005Y	2	30	...	...	...	$\gtrsim 0.5$	20.8 ± 0.1	...
P00066	2	18	...	...	...	$\gtrsim 0.6$	20.4 ± 0.1	...
P0007E	1	12	...	...	...	$\gtrsim 0.5$	20.6 ± 0.1	...
P0009S	1	8	...	...	...	$\gtrsim 0.4$	20.4 ± 0.1	...
P0009V	3	49	...	...	...	$\gtrsim 0.6$	19.71 ± 0.08	...
P000B1	2	16	...	...	...	$\gtrsim 0.3$	20.6 ± 0.2	...
P000B4	2	39	...	...	...	$\gtrsim 0.0$	19.81 ± 0.1	...
P000BH	1	16	...	...	...	$\gtrsim 0.4$	20.08 ± 0.1	...
P000CA	3	45	...	...	...	$\gtrsim 0.4$	20.3 ± 0.1	...
P000CK	1	9	...	...	...	$\gtrsim 0.4$	20.4 ± 0.1	...
P000DU	1	9	...	...	...	$\gtrsim 0.6$	20.5 ± 0.1	...
P000E2	3	48	...	...	...	$\gtrsim 0.5$	19.13 ± 0.06	...
P000EF	2	48	...	...	...	$\gtrsim 0.2$	19.6 ± 0.07	...
P000F5	3	143	...	...	...	$\gtrsim 0.5$	19.47 ± 0.07	...
P000FH	3	44	...	...	...	$\gtrsim 0.4$	20 ± 0.1	...
P000FI	2	28	...	...	...	$\gtrsim 0.6$	20.2 ± 0.1	...
P000HY	1	6	...	...	...	$\gtrsim 0.5$	20.7 ± 0.1	...
P000I0	3	120	...	...	...	$\gtrsim 0.6$	20.3 ± 0.1	...
P000I5	3	83	...	...	...	$\gtrsim 0.4$	19.92 ± 0.09	...
P000ID	1	15	...	...	...	$\gtrsim 0.5$	20.7 ± 0.1	...
P000II	1	15	...	...	...	$\gtrsim 0.6$	19.45 ± 0.07	...
P000JB	3	51	...	...	...	$\gtrsim 0.2$	19.09 ± 0.06	...

NOTE. — Columns: asteroids' designations, number of nights, number of images, geocentric (r) and heliocentric (Δ) distances, phase angle (α), lower limit on the lightcurve amplitude, mean magnitude, semi-major axis.

TABLE 5
CONTINUED

Designation	N_{nights}	N_{im}	r [AU]	Δ [AU]	α [deg]	Amp [mag]	$\langle R_{PTF} \rangle$ [mag]	a [AU]
P000JD	3	63	···	···	···	$\gtrsim 1.7$	19.59 ± 0.07	···
P000JF	2	54	···	···	···	$\gtrsim 1.3$	20.3 ± 0.1	···
P000JQ	3	60	···	···	···	$\gtrsim 0.3$	19.79 ± 0.09	···
P000JX	2	59	···	···	···	$\gtrsim 0.6$	19.96 ± 0.1	···
P000K1	1	23	···	···	···	$\gtrsim 0.8$	19.13 ± 0.06	···
P000K2	1	26	···	···	···	$\gtrsim 0.4$	18.99 ± 0.04	···
P000L7	1	15	···	···	···	$\gtrsim 2$	20.1 ± 0.1	···
P000LL	2	29	···	···	···	$\gtrsim 0.4$	20.2 ± 0.1	···
P000LX	3	79	···	···	···	$\gtrsim 0.5$	19.92 ± 0.1	···
P000M8	3	44	···	···	···	$\gtrsim 0.6$	20.2 ± 0.1	···
P000O8	2	14	···	···	···	$\gtrsim 0.9$	20.7 ± 0.1	···
P000OC	4	209	···	···	···	$\gtrsim 0.5$	19.5 ± 0.07	···
P000OJ	1	6	···	···	···	$\gtrsim 0.5$	20.5 ± 0.2	···
P000OX	1	6	···	···	···	$\gtrsim 0.7$	20.2 ± 0.1	···
P000Q3	2	36	···	···	···	$\gtrsim 0.4$	19.39 ± 0.07	···
P000S6	4	177	···	···	···	$\gtrsim 0.6$	18.62 ± 0.05	···
P000T0	2	46	···	···	···	$\gtrsim 0.4$	19.11 ± 0.06	···
P000TD	2	74	···	···	···	$\gtrsim 0.2$	19.46 ± 0.07	···
P000TG	1	15	···	···	···	$\gtrsim 0.7$	20.6 ± 0.1	···
P000TJ	2	28	···	···	···	$\gtrsim 0.4$	20.2 ± 0.1	···
P000TO	2	15	···	···	···	$\gtrsim 0.5$	20.7 ± 0.2	···
P000TP	3	55	···	···	···	$\gtrsim 0.6$	20.1 ± 0.1	···
P000VE	1	3	···	···	···	$\gtrsim 0.5$	20.8 ± 0.2	···
P000VM	2	34	···	···	···	$\gtrsim 0$	19.83 ± 0.08	···
P000VX	1	11	···	···	···	$\gtrsim 0.6$	20.5 ± 0.1	···
P000W0	1	5	···	···	···	$\gtrsim 0.7$	20.8 ± 0.2	···
P000W5	3	60	···	···	···	$\gtrsim 0.6$	19.26 ± 0.07	···
P000WG	1	4	···	···	···	$\gtrsim 0.7$	20.4 ± 0.1	···
P000WV	1	11	···	···	···	$\gtrsim 0.6$	21 ± 0.1	···
P000XD	1	5	···	···	···	$\gtrsim 0.5$	20.8 ± 0.2	···
P000XW	1	9	···	···	···	$\gtrsim 0.6$	20.5 ± 0.1	···
P000YT	2	35	···	···	···	$\gtrsim 1$	20.6 ± 0.2	···
P000Z7	1	5	···	···	···	$\gtrsim 1$	19.28 ± 0.09	···
P000ZA	2	15	···	···	···	$\gtrsim 0.3$	20.4 ± 0.1	···
P000ZB	3	60	···	···	···	$\gtrsim 0.4$	20.09 ± 0.1	···
P000ZD	2	32	···	···	···	$\gtrsim 0.6$	20 ± 0.1	···
P000ZF	1	15	···	···	···	$\gtrsim 0.4$	20.2 ± 0.1	···
P0011Y	2	22	···	···	···	$\gtrsim 1.6$	20.5 ± 0.1	···
P0012I	2	14	···	···	···	$\gtrsim 0.6$	20.5 ± 0.1	···
P0012N	3	41	···	···	···	$\gtrsim 0.5$	20.4 ± 0.1	···
P0012R	3	68	···	···	···	$\gtrsim 0.8$	20.2 ± 0.1	···
P0012X	3	24	···	···	···	$\gtrsim 0.3$	20.1 ± 0.1	···
P0013X	3	169	···	···	···	$\gtrsim 0.3$	19.4 ± 0.07	···
P0014P	1	10	···	···	···	$\gtrsim 0.5$	19.61 ± 0.07	···
P00154	1	13	···	···	···	$\gtrsim 0.2$	20.2 ± 0.1	···
P0015I	1	6	···	···	···	$\gtrsim 0.6$	19.04 ± 0.06	···
P0015N	1	7	···	···	···	$\gtrsim 0.6$	20.1 ± 0.1	···
P0018F	2	19	···	···	···	$\gtrsim 0.6$	20.9 ± 0.1	···
P0019B	1	8	···	···	···	$\gtrsim 0.2$	20.7 ± 0.2	···
P0019R	3	98	···	···	···	$\gtrsim 0.4$	20.2 ± 0.1	···
P001AK	3	22	···	···	···	$\gtrsim 0.3$	20.7 ± 0.1	···
P001AN	1	8	···	···	···	$\gtrsim 0.6$	21 ± 0.2	···
P001BR	2	56	···	···	···	$\gtrsim 0.3$	20.3 ± 0.1	···
P001BS	1	11	···	···	···	$\gtrsim 0.6$	20.9 ± 0.2	···
P001BT	1	7	···	···	···	$\gtrsim 0.4$	20.5 ± 0.1	···
P001DF	2	22	···	···	···	$\gtrsim 0.4$	19.46 ± 0.08	···
P001EM	2	25	···	···	···	$\gtrsim 0.4$	20.7 ± 0.1	···
P001EO	2	21	···	···	···	$\gtrsim 0.6$	19.8 ± 0.1	···
P001G5	2	31	···	···	···	$\gtrsim 0.5$	20.03 ± 0.1	···
P001G6	2	34	···	···	···	$\gtrsim 2$	20.5 ± 0.1	···
P001H4	2	22	···	···	···	$\gtrsim 0.4$	19.9 ± 0.1	···
P001HK	2	38	···	···	···	$\gtrsim 0.6$	19.73 ± 0.09	···
P001J9	2	14	···	···	···	$\gtrsim 0.6$	20.1 ± 0.1	···
P001JF	2	20	···	···	···	$\gtrsim 0.6$	20.2 ± 0.1	···
P001JW	1	13	···	···	···	$\gtrsim 1.4$	20.1 ± 0.1	···
P001LZ	3	51	···	···	···	$\gtrsim 0.8$	20.4 ± 0.1	···
P001M5	2	64	···	···	···	$\gtrsim 0.6$	20.3 ± 0.1	···
P001NS	1	17	···	···	···	$\gtrsim 0.5$	20.6 ± 0.1	···
P001NT	1	12	···	···	···	$\gtrsim 0.4$	20.4 ± 0.1	···
P001OF	1	6	···	···	···	$\gtrsim 0.5$	20.6 ± 0.2	···

NOTE. — Columns: asteroids' designations, number of nights, number of images, geocentric (r) and heliocentric (Δ) distances, phase angle (α), lower limit on the lightcurve amplitude, mean magnitude, semi-major axis.

TABLE 5
CONTINUED

Designation	N_{nights}	N_{im}	r [AU]	Δ [AU]	α [deg]	Amp [mag]	$\langle R_{PTF} \rangle$ [mag]	a [AU]
P001P1	1	7	···	···	···	$\gtrsim 0.3$	20.4 ± 0.1	···
P001T1	3	73	···	···	···	$\gtrsim 0.0$	19.95 ± 0.09	···
P001TQ	3	79	···	···	···	$\gtrsim 0.3$	20.4 ± 0.1	···
P001U2	2	69	···	···	···	$\gtrsim 0.4$	19.26 ± 0.05	···
P001U4	2	30	···	···	···	$\gtrsim 0.4$	19.9 ± 0.1	···
P001VG	2	28	···	···	···	$\gtrsim 0.9$	20.2 ± 0.1	···
P001VX	2	8	···	···	···	$\gtrsim 1.1$	20.6 ± 0.2	···
P001WD	3	41	···	···	···	$\gtrsim 1.6$	20.2 ± 0.1	···
P001X0	2	13	···	···	···	$\gtrsim 0.8$	20.8 ± 0.1	···
P001XV	1	5	···	···	···	$\gtrsim 1$	20.6 ± 0.2	···
P001XX	2	14	···	···	···	$\gtrsim 1.8$	20.3 ± 0.1	···
P001Y1	3	59	···	···	···	$\gtrsim 0.0$	20.4 ± 0.1	···
P001Y4	1	6	···	···	···	$\gtrsim 1.2$	20.8 ± 0.2	···
P001Y6	2	45	···	···	···	$\gtrsim 1.1$	20.3 ± 0.1	···
P001YQ	1	5	···	···	···	$\gtrsim 0.9$	20.5 ± 0.2	···
P001Z2	3	61	···	···	···	$\gtrsim 0.1$	20.5 ± 0.1	···
P001Z6	1	7	···	···	···	$\gtrsim 0.5$	20.5 ± 0.1	···
P0023W	3	30	···	···	···	$\gtrsim 0.7$	20.4 ± 0.1	···
P00254	1	6	···	···	···	$\gtrsim 0.4$	20.9 ± 0.2	···
P0025N	1	6	···	···	···	$\gtrsim 0.9$	20.7 ± 0.1	···
P00266	2	28	···	···	···	$\gtrsim 0.4$	20.08 ± 0.1	···
P00270	1	6	···	···	···	$\gtrsim 0.3$	20.7 ± 0.1	···
P0027A	3	57	···	···	···	$\gtrsim 0.3$	20.5 ± 0.1	···
P0027M	2	26	···	···	···	$\gtrsim 0.4$	20.4 ± 0.1	···
P0029N	1	12	···	···	···	$\gtrsim 0.6$	20.7 ± 0.2	···
P002D0	1	6	···	···	···	$\gtrsim 0.6$	20.9 ± 0.1	···
P002D4	1	8	···	···	···	$\gtrsim 0.6$	20.7 ± 0.2	···
P002DL	2	23	···	···	···	$\gtrsim 0.5$	20.6 ± 0.1	···
P002DQ	3	23	···	···	···	$\gtrsim 0.4$	20.8 ± 0.2	···
P002E3	1	6	···	···	···	$\gtrsim 0.4$	20.8 ± 0.1	···
P002EB	3	33	···	···	···	$\gtrsim 0.6$	20.4 ± 0.1	···

NOTE. — Columns: asteroids' designations, number of nights, number of images, geocentric (r) and heliocentric (Δ) distances, phase angle (α), lower limit on the lightcurve amplitude, mean magnitude, semi-major axis.

Table 6 can be found in its entirety here:
$http://wise-obs.tau.ac.il/\sim david/PTF/Data/Polishook\_EtAl\_2012\_MNRAS\_PTF\_Asteroids\_Table6$
Columns: asteroids designations, PTFs field and CCD, JD [days], RA [degrees], Dec [degrees], calibrated magnitude [mag], air mass, images background count and FWHM [arcsec]. The last six parameters are given only for objects with known orbital parameters: geocentric (r) and heliocentric (Δ) distances [AU], phase angle (α) [degrees], semi-major axis [AU], eccentricity and inclination [degrees].